



HAL
open science

Geological architecture and history of the Antigua volcano and carbonate platform: Was there an Oligo–Miocene lull in Lesser Antilles arc magmatism?

Leny Montheil, Mélody Philippon, Jean-Jacques Cornée, Marcelle Boudagher-Fadel, Douwe J.J. van Hinsbergen, Pierre Camps, Marco Maffione, Franck Audemard, Brechtje Brons, Koen J.R. van der Looij, et al.

► To cite this version:

Leny Montheil, Mélody Philippon, Jean-Jacques Cornée, Marcelle Boudagher-Fadel, Douwe J.J. van Hinsbergen, et al.. Geological architecture and history of the Antigua volcano and carbonate platform: Was there an Oligo–Miocene lull in Lesser Antilles arc magmatism?. Geological Society of America Bulletin, 2022, 10.1130/B36465.1 . hal-03838192

HAL Id: hal-03838192

<https://hal.science/hal-03838192v1>

Submitted on 3 Nov 2022

HAL is a multi-disciplinary open access archive for the deposit and dissemination of scientific research documents, whether they are published or not. The documents may come from teaching and research institutions in France or abroad, or from public or private research centers.

L'archive ouverte pluridisciplinaire **HAL**, est destinée au dépôt et à la diffusion de documents scientifiques de niveau recherche, publiés ou non, émanant des établissements d'enseignement et de recherche français ou étrangers, des laboratoires publics ou privés.

1 **Geological architecture and history of the Antigua**
2 **volcano and carbonate platform: was there an Oligo-**
3 **Miocene lull in Lesser Antilles arc magmatism?**

4 Leny Montheil¹, Mélody Philippon², Jean-Jacques Cornée², Marcelle Boudagher-
5 Fadel³, Douwe J.J. van Hinsbergen⁴, Pierre Camps¹, Marco Maffione⁶, Franck
6 Audemard⁵, Brechtje Brons⁴, Koen J.R. Van der Looij⁴, Philippe Münch¹

7 ¹ *Géosciences Montpellier, Université de Montpellier-CNRS-Université des Antilles),*
8 *34095 Montpellier Cedex 05, France. leny.montheil92@gmail.com;*
9 *pierre.camps@umontpellier.fr; philippe.munch@umontpellier.fr*

10 ² *Géosciences Montpellier (Université de Montpellier-CNRS-Université des Antilles),*
11 *97159 Pointe-à-Pitre, France. melody.philippon@univ-antilles.fr; jean-*
12 *jacques.cornee@umontpellier.fr*

13 ³ *Office of the Vice-Provost (Research), University College London, 2 Taviton Street,*
14 *London WC1H 0BT, UK. m.fadel@ucl.ac.uk*

15 ⁴ *Department of Earth Sciences, Utrecht University, Princetonlaan 8A, 3584 CB*
16 *Utrecht, the Netherlands. D.J.J.vanHinsbergen@uu.nl; b.brons@students.uu.nl;*
17 *k.j.r.vanderlooi@students.uu.nl*

18 ⁵ *FUNVISIS, Caracas, Venezuela. faudemard@gmail.com*

19 ⁶ *School of Geography, Earth and Environmental Sciences, University of*
20 *Birmingham, B15 2TT, UK. M.Maffiane@bham.ac.uk*

21

22 **Keywords:** Lesser Antilles subduction, arc, magmatic lull and flareup, Antigua,
23 tectonics, radiochronology, biostratigraphy.

24

25 **Corresponding author :** Leny Montheil, leny.montheil92@gmail.com

26

27

28

29 **ABSTRACT**

30 Since the acceptance of plate tectonics, the presence of calc-alkaline magmatic
31 rocks is recognized as evidence of subduction. But under specific geodynamic
32 circumstances, subduction may occur without generating magmas. Here, we
33 investigate the Cenozoic northern Lesser Antilles arc where, from sparsely exposed
34 magmatic records, Eocene-Oligocene and Pliocene magmatic flare-ups and a Miocene
35 lull were postulated. Nevertheless, most of the arc is submarine, so it is challenging to
36 discern lulls and flare-ups from sampling bias. We make a review of the magmatic
37 evidences exposed onshore in the Lesser Antilles and investigate in detail the island
38 of Antigua that exposes an Eocene to Miocene volcanic sequence and platform
39 carbonate series that coincide with the postulated lull. By combining,
40 lithostratigraphic analysis, structural mapping, $^{40}\text{Ar}/^{39}\text{Ar}$ geochronology, and
41 biostratigraphy we refine the magmatic history of the island and date the arrest of
42 extensive arc magmatism at 35 Ma, with minor activity until 27 Ma. No magmatic
43 products are interleaved with the platform sequence until the latest Oligocene,
44 confirming a lull in northern Lesser Antilles arc magmatism, that may have lasted ~
45 20 Ma. We propose that the magmatic activity contributed to the paleo-(bio-
46)geographical evolution of the Eastern Caribbean region with crustal thickening
47 during flareup favouring the rise of terrestrial pathways and thermal subsidence
48 during lull responsible for its demise.

49 Fault kinematic analysis together with anisotropy of magnetic susceptibility
50 suggests that magmatic arrest is not associated with a change in stress field during
51 Oligocene. We speculate that slab flattening triggered by progressive curvature played
52 a role in the temporal shut-down of the northern Lesser Antilles arc.

53

54 **INTRODUCTION**

55 Active volcanic arcs and associated calc-alkaline magmatic rocks are recognized as
56 closely associated with, and being the result of, modern subduction zones (e.g.,
57 Tatsumi et al., 1983; Davies and Stevenson, 1992; Pearce and Peate, 1995). Based on
58 that observation, geological records of volcanic arcs have become widely used as
59 argument to date and reconstruct contemporaneous paleo-subduction zones (e.g., Li et
60 al., 2008; Merdith et al., 2021; Cawood et al., 2009). But is the reverse also true ? Is
61 absence of arc magmatism evidence against subduction?

62 Worldwide, spatial and temporal lulls in magmatism are identified with the absence of
63 calc-alkaline magmas in the rock record. Such gaps are observed in the trans-Mexican
64 belt (Ferrari et al., 2001, 2012), the Andes (Kay and Coira, 2006; Gutscher et al,
65 2000; Rosenbaum et al., 2021), the archetypal Cascade arc of the western USA
66 (Glazner, 2004), the Nankai trough near Japan (Cross and Pilger, 1982; McGeary et
67 al, 1985), Taiwan (Yang et al., 1996), Sumatra (Zhang et al., 2019), and in Tibet (Ma
68 et al., 2022). In the western European Alps, subduction of the Tethys ocean did not
69 produce long-lasting magmatic activity (e.g., McCarthy et al., 2020). Such paucity of
70 magmatic evidence is typically explained by specific variations in geodynamical
71 parameters that may affect the downgoing plate and the upper-plate, such as flat-slab
72 subduction (McGeary et al, 1985, van Hunen et al., 2002, Martinod et al, 2013, Zhang
73 et al., 2019; Ma et al., 2022), subduction of hyperextended, dry mantle (McCarthy et
74 al., 2020), or changes in convergence rates (Cross and Pilger, 1982), but not as an
75 absence of subduction.

76 In the Eastern Caribbean, the Lesser Antilles region host an arc for which magmatic
77 flare-ups and lulls has been postulated (Briden et al., 1978; Bouysse and Westercamp,
78 1990). At first-look, the Lesser Antilles arc is a textbook example of ocean-ocean

79 subduction (e.g., MacDonald et al., 2000). The N-S trending Lesser Antilles trench
80 accommodate 2 cm/year of westward motion of North and South America relative to
81 the overriding Caribbean plate (Pindell and Dewey, 1982; Boschman et al., 2014,
82 Symithe et al., 2016) (Fig. 1). Marine magnetic anomalies in the Cayman Trough, that
83 forms a pull-apart basin on the Caribbean-North American plate boundary,
84 documented constant and stable westward plate motion since 50 Ma (Leroy et al.,
85 2000). This subduction is associated with a currently active, well-developed modern
86 volcanic arc that consists of 17 active volcanoes forming islands spread over ~800
87 km. Nevertheless, the arc rocks exposed on these islands are mainly recent (Pliocene
88 to Present-day) and the magmatic record shows significant breaks in volcanism along
89 sections of the arc during both the Late Paleogene and Miocene, especially in the
90 northern part of the arc (Brown et al., 1977; Briden et al. 1979; Bouysse and
91 Westercamp, 1990; MacDonald et al., 2000; Legendre et al. 2018; Noury et al., 2021).
92 In the northern Lesser Antilles, older arc rocks are confined to the islands of the
93 ‘Limestone Caribbees’, that are located in the forearc of the modern arc (Fig. 1, Fig.
94 2, Table 1). The Limestone Caribbees contain well-developed Eocene (~45 Ma) to
95 early Oligocene (~28 Ma) volcanic records, overlain by platform carbonates. From
96 the period between 28 Ma to 20 Ma, only sparse records of magmatic activity have
97 been reported from the northeastern branch of the Lesser Antilles arc (Briden et al.,
98 1978, Legendre et al., 2018, Cornée et al., 2021, Noury et al., 2022) (Fig. 2, Table 1).
99 From 20 Ma to 4 Ma, no record of magmatic activity is reported in the Northern
100 Lesser Antilles (Fig. 2, Table. 1). This interval could represent a lull in magmatism or
101 simply be a sampling bias as exposure are sparsely dispersed on islands. Miocene
102 volcanic record could also be buried below younger volcanoes or located offshore.

103 An answer to these questions may come from Antigua, that displays a
104 magmatic unit whose age was previously estimated from Oligocene to Miocene based
105 on K-Ar whole rock analysis (Nagle et al., 1976; Briden et al., 1978) and where the
106 only complete Oligocene to Miocene sedimentary sequence of the Limestone
107 Caribbees is preserved.

108 Uncertainties on the K-Ar ages, that are partly rejuvenated by a hydrothermal
109 event (Gunn and Roobol, 1976; Briden et al., 1978), on the age and thickness of the
110 sedimentary sequence (Mascle and Westercamp, 1983; Multer et al., 1986; Weiss,
111 1994) and the absence of structural data and of a description of the tectonic
112 architecture of the island lead to uncertainties on the timing of the geological events
113 that affected the island and consequently on the age of the arrest of the northern
114 Paleogene Lesser Antilles arc (even questioning the existence of its arrest).

115 In that perspective, we constrain the magmatic and stratigraphic architecture
116 and evolution of the island, by developing (1) the detailed lithostratigraphy record of
117 the island, in which we analysed the temporal and spatial relationships between the
118 previously identified lithological units; (2) a first mapping and analysis of the tectonic
119 structures deforming the lithological units; (3) an updated geological map according
120 to our lithostratigraphy and structural analysis. We aim to refine the duration of
121 magmatism and the duration and depositional setting of sedimentary rocks (which
122 may or may not overlap) by establishing (4) age estimates of key volcanic and
123 intrusive units using $^{40}\text{Ar}/^{39}\text{Ar}$ geochronology and (5) an updated facies analysis and
124 foraminiferal biostratigraphy of the marine units. To estimate whether changes in
125 magmatism correlate with tectonic changes, we perform on the scale of Antigua (6) a
126 kinematic analysis using small-scale syn- and post- depositional faults; and (7) an
127 anisotropy of the magnetic susceptibility (AMS) study to complement the structural

128 analysis and estimate the stress field, and changes therein, that existed during
129 sedimentation. Finally, we aim at putting our results in most recent regional structural,
130 stratigraphic and paleo-geographic frameworks (Philippon et al., 2020a; Marivaux et
131 al., 2020; Cornée et al., 2021) by providing land-sea correlations using seismic lines
132 to the west and south of Antigua acquired during the Antilles IV oceanographic cruise
133 (Bouysse and Mascle, 1994). We will use our results to evaluate the presence and
134 duration of a lull in Lesser Antilles magmatism and discuss our results in terms of
135 possible geodynamic triggers for anomalous magmatism.

136 **GEOLOGICAL SETTINGS**

137 **Regional setting**

138 The Lesser Antilles arc developed above a west-dipping subduction zone that
139 accommodates the convergence between the Caribbean upper plate and the
140 downgoing North and South America plates. The plate boundary between the North
141 and South American plates is diffuse, as relative motion between the two is minor
142 (e.g., Pindell and Kennan, 2009; Fig. 1). To the north and south, the Caribbean plate
143 boundary changes to E-W trending transforms, sinistral in the north and dextral in the
144 south (Pindell and Kennan, 2009; Fig. 1). The transition is abrupt in the south and
145 accommodated by a slab tear but gradual in the north along a curved plate boundary
146 overlying a curved, amphitheater-shaped slab with a north(west)ward increase in
147 subduction obliquity (Govers and Wortel, 2005; van Benthem et al., 2013; 2014) (Fig.
148 1). This plate configuration developed around 60-40 Ma ago when the Caribbean
149 plate motion relative to the Americas changed from NE-ward to E-ward (Boschman et
150 al., 2014; Montes et al., 2019). Before that, the Eastern Caribbean plate boundary
151 consisted of an oblique subduction at the origin of the Great Caribbean Arc that

152 extended from Cuba to the south of the Aves Ridge (Fox et al., 1971; Bouysse et al.,
153 1985; Christeson et al., 2008; Neill et al., 2011, Allen et al., 2019, Padron et al., 2021,
154 Fig. 1). After the kink, the subduction became orthogonal and the arc jumped
155 eastward toward the Limestones Caribbees.

156 At regional scale, a north-south morpho-structural dichotomy is observed
157 along the curved Lesser Antilles trench: the southern back-arc region hosts the
158 Eocene Grenada basin with a flat bathymetry and a mean depth of 2800 m and thin
159 oceanic crust (Garrocq et al. 2021, Padron et al., 2021). To the north, the seafloor is
160 rough, mean bathymetry is 1400 m, and the arc crust is thicker (Schlaphorst et al.,
161 2018). The Northern Lesser Antilles region, hosts a middle to late Eocene fold and
162 thrust belt (Philippon et al., 2020a) in which subsequently, the trench-parallel
163 Kalinago extensional basin opened in the late Eocene to early Oligocene (Bouysse et
164 al., 1990; Legendre et al., 2018; Philippon et al., 2020a; Cornée et al., 2021; Fig. 1).

165 From the late Oligocene to middle Miocene, the Northern Lesser Antilles forearc
166 became deformed by V-shaped extensional, perpendicular to the trench basins that
167 opened from late Oligocene to middle Miocene time (Fig. 1). That may suggest
168 intensification of the trench curvature (Philippon et al., 2020b; Boucard et al., 2021).
169 These basins are crosscut by trench-parallel normal faults since middle Miocene that
170 accommodate fore-arc subsidence (Boucard et al., 2021).

171 Offshore investigations in the southern Kalinago basin and its extension south of
172 Antigua island (Willoughby sub-basin) showed that the sedimentary infilling was
173 composed of three megasequences (MS) separated by regional unconformities
174 (Sequence Boundaries, SB) : a late Oligocene to early Miocene megasequence (MS4)
175 resting above a deformed basement and topped by the early- middle Miocene major
176 erosional surface (SB4) indicative of a regional uplift; middle to present day

177 megasequences (MS5 to MS 6-7) representative of a subsidence of the Kalinago and
178 Willoughby basins (Cornée et al., 2021; Fig. 11, Appendix 3). No conic structures or
179 chimneys, that could have been representative of a fossil volcanic activity were found
180 on seismic lines.

181 The present-day Lesser Antilles magmatic arc consists primarily of calc-
182 alkaline volcanoes forming islands from Grenada in the south to Saba in the north
183 (Macdonald, 2000) (Fig. 1). These islands span a trench-parallel arc, with a north-
184 westward kink at the latitude of Martinique (Fig. 1).

185 To the south, the Pliocene to present-day arc is superimposed on older arc
186 rocks. In Grenada and the Grenadines, these rocks are upper Eocene to Miocene calc-
187 alkaline dykes, volcanic arc rocks and volcanoclastic deposits (Briden et al., 1979;
188 Westercamp et al., 1985; Andréieff et al., 1987; Speed et al., 1993; Donovan et al.,
189 2003; Rojas-Agramonte et al., 2017; White et al., 2017) (Fig. 2, Table 1). In
190 Dominica, Martinique, and Sainte-Lucia, older arc rocks consist of well-developed
191 latest Oligocene to Miocene volcanics (Le Guen de Kerneizon et al., 1983,
192 Westercamp et al., 1985, Briden et al., 1979, Germa et al., 2011, Smith et al., 2013)
193 (Fig. 2, Table 1).

194 In the north, the onset of recent arc volcanoes occurred during the
195 Pliocene to present-day on Saba, St-Eustatius, St-Kitts and Nevis, Monserrat, and
196 Guadeloupe (Baker, 1984; Defant et al., 2001; Samper et al., 2007; Hatter et al., 2018;
197 Favier et al., 2019). These eruptive centers are located on the western shoulder of the
198 Kalinago basin, 50 to 20 km westward from the older eruptive centers preserved in
199 the NW-trending ‘Limestones Caribbees’ islands (St-Martin, St-Barthélemy, Antigua)
200 on the eastern shoulder of the Kalinago basin (Fig. 1).

201 The Limestone Caribbees host platform carbonates overlying extinct volcanoes, that
202 are preserved in flat bathymetric high (Anguilla and Antigua Banks). These banks are
203 bounded to the east by V-shaped basins (Fig. 1). On St-Martin, arc volcanism
204 developed an Eocene volcanoclastic series (Dagain et al., 1989) intruded by a 29 Ma
205 granodioritic pluton and associated dykes and sills (Noury et al., 2021), and last
206 magmatic activity is represented by a submarine volcanic breccia of 24.4 Ma (Cornée
207 et al., 2021, Fig. 2, Table 1). In St-Barthélemy, magmatic rocks consist of submarine
208 tholeiitic and calc-alkaline lavas (45 to 39 Ma), granodioritic plutons (33.5 to 30 Ma)
209 and local tholeiitic lavas (24.5 Ma, Legendre et al., 2018; Philippon et al., 2020a;
210 Fig.1, Table 1). On Antigua, current dating (K-Ar whole rock analysis, Nagle et al.,
211 1976; Briden et al., 1979) supports arc magmatism from the Late Eocene to Miocene
212 and comprises plutonic and volcanic calc-alkaline rocks (Basal Volcanic Suite) and an
213 Oligocene volcanoclastic series (Central Plain Group, Gunn and Roobol, 1976; Briden
214 et al., 1979; Mascle and Westercamp, 1983) (Fig. 2, Table 1).

215 **Geology of Antigua**

216 The first geological study of the lithologies of Antigua by Vaughan (1919)
217 described coral associations and larger benthic foraminifera. Martin-Kaye (1959)
218 subdivided the island in three NW-SE trending geological units, the Basal Volcanic
219 Suite (BVS), the Central Plain Group (CPG) and the Antigua Formation (Fig. 3).

220 The Basal Volcanic Suite is a mountainous region exposed on the west side of
221 the island, which includes the island's highest point (Mont Obama, 402 m). The suite
222 consists of lava flows and pyroclastic rocks, dykes, and domes of predominantly
223 basaltic, andesitic, and dacitic compositions and with island-arc type geochemical
224 signature (Christman, 1973; Gunn and Roobol, 1976; Fig. 3). Basaltic dykes are also
225 found crosscutting the topmost stratigraphic units (CPG and Antigua Fm.) and are

226 thus considered as the last magmatic pulses exposed on the island (Martin-Kayes,
227 1959, 1969; Fig.2). Whole rock K-Ar analyses for volcanic rocks of the BVS gave
228 ages ranging between 38.5 ± 2 Ma (middle Eocene) and 20 Ma ? (minimum age, early
229 Miocene) (Nagle et al., 1976; Briden et al., 1979).

230 The Central Plain Group is described as a ~1500m of terrestrial volcanoclastic
231 rocks (conglomerates, sandstones, mudrocks, tuffites) derived from volcanism and the
232 erosion of the Basal Volcanic Suite (Masclé and Westercamp, 1983; Multer et al.,
233 1986; Weiss, 1994). These volcanoclastic rocks are interbedded with lacustrine
234 limestones, which contain petrified wood, charophytes, ostracods, and freshwater
235 gastropods (Brown and Pilsbry, 1914; Trechman, 1941; Martin-Kayes, 1959, 1969;
236 Masclé and Westercamp, 1983; Weiss, 1994; Donovan et al., 2014, Fig. 3). Thomas
237 (1942) and Martin-Kayes (1959, 1969) also suggested that there may be patches of
238 marine carbonates interbedded with the CPG (e.g., the Seaforth limestone, Fig. 3) that
239 they interpreted as episodic marine invasions.

240 The Antigua Fm. is composed of carbonate deposits overlying the CPG, in which
241 volcanic deposits have not been recognized. It comprises numerous coral patches and
242 associated bioclastic carbonate deposits, upward and laterally changing into deeper
243 marine carbonate deposits in the east (e.g., Martin-Kayes, 1959, 1969; Persad, 1969;
244 Masclé and Westercamp, 1983; Multer et al., 1986; Weiss, 1994). The estimated
245 thickness of the Antigua Fm is 350 to 550 m (Masclé and Westercamp, 1983). Based
246 on the study of larger benthic foraminifera, planktonic foraminifera, ostracods, and
247 calcareous nannofossils, the age of the Antigua Fm has been estimated as Late
248 Oligocene (Chattian) (Vaughan, 1919; Van den Bold, 1966; Martin- Kaye, 1959,
249 1969; Persad, 1969; Masclé and Westercamp, 1983), consistent with five strontium
250 isotope ages ranging from 26 to 28 Ma (Robinson et al., 2017, Fig. 3) and with recent

251 preliminary age determinations of Cornée et al. (2021). Previous geological studies
252 did not investigate the tectonic architecture or structural history of Antigua.
253 The three units composing the island are affected by sub-greenschist hydrothermal
254 alteration that could be responsible for rejuvenation of K-Ar ages (Briden et al. 1978).
255 Gunn and Roobol, (1976) observed albitised plagioclases and chloritised
256 orthopyroxenes and groundmass in the Basal Volcanic Suite. In the Central Plain
257 Group, bright green chloritised tuffites were described by Martin-Kaye (1959, 1969)
258 and Jackson et al. (2013). In the Antigua Fm, this alteration phase is found in the form
259 of silicified limestones (Strang et al., 2018).

260

261 **METHODS**

262 **Field investigation**

263 Three field campaigns (2018, 2019, and 2020) were conducted to investigate the
264 tectono-magmatic history of Antigua. Exposure within the interior of the island is
265 poor due to thick alluvial, colluvium, or vegetation cover. Exposure is most abundant
266 along the coast, even though numerous private properties hampered a full remapping
267 of some coastal portions. Nevertheless, we updated the geological map by mapping
268 the first-order lithostratigraphic units and regional structures (unconformities, faults,
269 dykes), and investigating the relations between units (Fig. 3).

270 Because the Antigua formation outcrops are isolated, we coupled microfacies and
271 biostratigraphy with lithostratigraphy to reconstruct the general sedimentary
272 organization (Fig. 4, Appendix 1) and paleo-environments (Fig. 10). We logged eight
273 sedimentary sections in the Central Plain Group (CPG) and ten in the Antigua Fm.
274 (Fig. 4, Appendix 1) and used dated isolated exposures from road cuts or along the

275 seashore (e.g., Galleon, Military Camp, Marble Hill, Fort James, Nelson Dockyard,
276 Piggots, Willoughby Bay), continuous cross-sections along the shoreline (e.g., Half
277 Moon Bay, Devil's Bridge, Pigeon Beach) and quarries (Burma, Newfield, Pares,
278 Parnham) (Fig. 3, Fig. 4). We collected some 400 structural measurements
279 (bedding orientations, faults, striaes) and reported these on the map (Fig. 3,
280 Appendix 4).

281 $^{40}\text{Ar}/^{39}\text{Ar}$ geochronology

282 For $^{40}\text{Ar}/^{39}\text{Ar}$ geochronology, we collected samples from volcanic and igneous
283 rocks of the BVS (Fig. 3). To understand the magmatic evolution of the island, we
284 collected all types of magmatic material that were recognized in the island, targeting
285 the least altered outcrops. Samples consist on an andesitic lava (ANT 20.4, Fig. 5C)
286 crosscut by a rhyolitic dyke (DWB-B, Fig. 5C), a dacitic dome (ANT 6.8, Sugar Hill)
287 a quartz-dioritic pluton (ANT 20.8, Old Road) and two mafic dykes, one crosscutting
288 the CPG (ANT 20.12, Fig. 3, Fig. 5B) and the other that pierce the base of the
289 Antigua Fm (ANT 20.6, Fig. 3). $^{40}\text{Ar}/^{39}\text{Ar}$ step-heating analyses were performed at
290 Géosciences Montpellier (France, detailed methodology in Appendix 5). Raw data of
291 each step and blank were processed and ages were calculated using the ArArCALC
292 software (Koppers, 2002). Ages are statistically analyzed in two ways: ^{39}Ar released
293 spectra and inverse isochrones. Plateau ages are calculated from at least three
294 consecutive ^{39}Ar release steps comprising up to 50% of total $^{39}\text{Ar}_K$ released and
295 overlapping at the 2σ -confidence level (Fleck et al., 1977). Isochrone ages are
296 accepted when mean square weighted deviation (MSWD) is close to 1 and the
297 $^{40}\text{Ar}/^{36}\text{Ar}$ intercept close to the $(^{40}\text{Ar}/^{36}\text{Ar})_{\text{atm}}$ value. All results are given at the 2σ
298 uncertainty.

299 **Microfacies and biostratigraphy**

300 For microfacies and fossil content determination, 35 thin sections were
301 analyzed from the carbonate rocks of the Antigua Fm. and ten from volcanoclastic
302 rocks and lacustrine limestones of the CPG, collected from the 18 logged sections
303 (Fig. 4, Appendix 1). The microfacies were associated to a depositional environment
304 following the classification of Wright and Burchette (1996) and Flügel (2010),
305 supplemented by the larger benthic foraminiferal content (BouDagher-Fadel, 2018a)
306 (Fig. 10, Appendix 2). The biostratigraphic analyses were only carried out for the
307 marine Antigua Formation (the CPG only contains undatable freshwater gastropods),
308 and were based on a complete inventory of larger benthic and planktonic foraminifera
309 taxa identified in the thin sections. We used the zonal calibrations of BouDagher-
310 Fadel (2015, 2018b) for the foraminifera, calibrated against the time scale of
311 Gradstein et al. (2012).

312 **Fault analysis**

313 We employed the right dihedral methods to inverse fault kinematics and interpret the
314 paleo-stress tensor using WinTensor software (Angelier, 1979; Delvaux and Sperner,
315 2003). WinTensor allows the rotational optimization of the obtained tensor by
316 performing iterative tests of tensors to minimize a misfit function. We perform these
317 inversions with sets of data consisting of fault strike, dip, plunge of the striations and
318 bedding offsets (Appendix 4). The quality of inversion is given by QRw (world
319 stress map quality criteria) ranging from A (good) to E (poor) depending of the
320 amount of data used for the inversion (n), the ratio between the amount of data used
321 for the inversion over the amount of input data (n/nt), deviation between observed and
322 theoretical slip direction (α_w), the sense of slip confidence level (Cl_w) and the type of
323 structure (fault, fracture, shear zone).

324 **Anisotropy of the magnetic susceptibility (AMS)**

325 To supplement fault kinematics analysis, we used anisotropy of the magnetic
326 susceptibility (AMS) to determine the petrofabric of samples of the CPG and of the
327 Antigua Fm. and determine the direction of tectonic paleo-strain. We drilled 71
328 paleomagnetic cores of fine-grained rocks over 8 sites (Fig. 9A). Samples were
329 collected with a petrol-powered, water-cooled drill and oriented with a magnetic
330 compass. The local magnetic declination (14° W in January 2020) was corrected on
331 all samples. Non-demagnetized standard specimens were measured using an AGICO
332 KLY-3S Kappabridge at the Geosciences Montpellier palaeomagnetic laboratory.
333 AMS is defined by an ellipsoid with the principal axes $k_{\max} > k_{\text{int}} > k_{\min}$ used as strain
334 indicator (Jelinek, 1978; Parés et al., 1999; Maffione et al., 2015). Undeformed
335 sediments display a so-called sedimentary fabric where k_{\max} and k_{int} are dispersed
336 within the plane of magnetic foliation (F), which is parallel to the sedimentary
337 stratification, and k_{\min} is the pole to the bedding plane. A tectonic fabric can overprint
338 the sedimentary one, and produce a magnetic lineation (L) by aligning the k_{\max} axes
339 parallel to the maximum axis of stretching (σ_3). In this study we have used the
340 magnetic lineation as a paleo-strain proxy to determine the nature and direction of the
341 tectonic strain. The AMS parameters were evaluated using ANISOFT 5.1 software
342 according to Jelinek statistics (Jelinek, 1978; Chadima et al., 2020).

343

344 **RESULTS**

345 **$^{40}\text{Ar}/^{39}\text{Ar}$ geochronology of the BVS**

346 The Basal Volcanic Suite (BVS) crops out in the southwest of the island and is
347 mainly composed of andesitic lavas and pyroclastic deposits. These are crosscut by
348 rhyolitic dykes (Fig. 5C) and intruded by a dacitic dome at Sugar Hill and at Seaforth

349 Bay (Fig. 3). At the site of Old Road, a small stock of quartzitic diorite, previously
350 described by Christmann (1973) is intruded by ENE-WSW rhyolitic dykes similar in
351 appearance with the one crosscutting the andesitic lavas (Fig. 5C, 5D). To the south-
352 east, at Nelson Dockyard, mafic dykes intrudes the CPG. To the northeast and
353 southeast (Devil's Bridge) similar dyke are found intruding the Antigua Fm. (Fig.3,
354 Fig. 5A, 5B). No consistent bedding dip is apparent in the BVS; the pyroclastic rocks
355 have bedding that vary between 0 to 30° around local eruptive centers (Fig. 3).

356 The andesitic lava (sample ANT20.4) yields a plateau age of 18.57 ± 1.26 Ma
357 with 82.07 % of Ar released (Fig.8, Table 2). Individual steps show large errors,
358 especially for low temperature degassing steps, resulting from high atmospheric
359 contamination. Consequently, all data cluster along the ordinate axis of the inverse
360 isochron diagram. The inverse isochron calculations for the steps corresponding to the
361 plateau yielded a concordant age of 19.74 ± 2.46 Ma with MSWD = 1.52 for an initial
362 $^{40}\text{Ar}/^{36}\text{Ar}$ ratio of 297.8 ± 1.5 indicating that the trapped $^{40}\text{Ar}/^{36}\text{Ar}$ is indistinguishable
363 from atmospheric $^{40}\text{Ar}/^{36}\text{Ar}$.

364 The rhyolitic dyke (sample DWB-B) that crosscuts the andesite lava flow
365 (sample ANT20.4) yields a hump-shaped spectrum with a mini-plateau age
366 (cumulative ^{39}Ar released ~40 %) of 35.32 ± 0.16 Ma. The inverse isochron
367 calculations for the steps corresponding to the mini-plateaus yielded concordant ages
368 of 35.06 ± 0.61 Ma (MSWD = 1.93, initial $^{40}\text{Ar}/^{36}\text{Ar}$ ratio of 301.9 ± 7.3) with the
369 trapped $^{40}\text{Ar}/^{36}\text{Ar}$ indistinguishable from atmospheric $^{40}\text{Ar}/^{36}\text{Ar}$. The low and high
370 temperature degassing steps yield younger ages between 10 and 15 Ma and exhibit
371 compositions poorer in ^{40}Ar and richer in ^{38}Ar than the central part, indicating that
372 they correspond to a secondary phase (Fig. 8, Table 2).

373 Plagioclase populations from the dacitic dome of Sugar Hill, previously dated

374 with K-Ar geochronology at 20.8 Ma (Nagle et al., 1976, Fig. 3), yield a plateau age
375 of 29.76 ± 0.22 Ma for the central part of the spectra corresponding to 68.59% of the
376 ^{39}Ar released. The inverse isochron age of 29.74 ± 0.62 Ma is concordant with an
377 $\text{MSWD} = 2.03$ and an initial $^{40}\text{Ar}/^{36}\text{Ar}$ ratio of 298.9 ± 9.4 , indicating that the trapped
378 $^{40}\text{Ar}/^{36}\text{Ar}$ is indistinguishable from atmospheric $^{40}\text{Ar}/^{36}\text{Ar}$ (Fig. 8, Table 2).

379 Analysis of the plagioclase population of the quartz diorite (ANT 20.8) yields
380 a staircase spectrum without a plateau ranging from 10 Ma for low temperature
381 degassing steps to 28 Ma at high temperature. The total fusion age is 22.88 ± 0.29
382 Ma. To aid interpretation of the measured spectra and the thermal history, we
383 performed an inverse modelling of the $^{40}\text{Ar}/^{39}\text{Ar}$ spectra of the plagioclase population
384 from the dioritic pluton with QTQt software (Gallagher, 2012). The inverse QTQt
385 model for the plagioclase $^{40}\text{Ar}/^{39}\text{Ar}$ spectrum suggests that the diorite sample
386 underwent a steady cooling at a rate of $\sim 5^\circ/\text{Ma}$ since ~ 25 Ma (Fig. 8).

387 Despite a large error on individual steps related to atmospheric contamination,
388 analysis of the groundmass of the basaltic andesite dyke crosscutting the Central Plain
389 Group (ANT20.12) yields a plateau age of 27.03 ± 1.89 Ma corresponding to 90.99 %
390 of the ^{39}Ar released (Fig. 8, Table 2). The inverse isochron yields a concordant age of
391 27.73 ± 2.94 Ma with an $\text{MSWD} = 0.48$ and an initial $^{40}\text{Ar}/^{36}\text{Ar}$ ratio of 297.3 ± 3.2
392 indistinguishable from atmospheric ratio. Low-temperature individual degassing steps
393 show larger errors and yield younger ages (10 to 20 Ma).

394 For the basaltic andesite dyke intruding the Antigua Fm (ANT 20.6) we
395 analyzed both plagioclase and groundmass populations. The plagioclase analysis
396 yields a plateau age of 30.50 ± 0.70 Ma with a large error on degassing steps
397 corresponding to 97.98 % of the ^{39}Ar released (Fig. 8, Table 2). Calculated inverse
398 isochron show indistinguishable trapped and atmospheric $^{40}\text{Ar}/^{36}\text{Ar}$ and an age of

399 30.57 ± 0.81 Ma with MSWD = 0.74 for an initial $^{40}\text{Ar}/^{36}\text{Ar}$ ratio of 297.7 ± 5.4 .
400 Analysis on the groundmass population did not yield a plateau and a hump-shaped
401 spectrum with younger low and high temperature individual steps (~15 Ma) with a
402 poorer ^{40}Ar and richer ^{38}Ar composition. However, the total fusion age obtained on
403 groundmass (30.54 ± 0.27 Ma) is concordant with the plateau age obtained from
404 plagioclase population analysis.

405

406 **Lithostratigraphy, microfacies and biostratigraphy**

407 Central Plain Group

408 The CPG comprises various terrestrial clastic rocks, lacustrine limestones,
409 volcanoclastic mud and debris flows and conglomerates interpreted as alluvial fan
410 deposits, volcanoclastic clay-rich deposits, tuffites, and lapilli-rich beds. These are
411 well exposed at St-John, Corbison, to the NW, and at the site of All Saints, in the
412 central part of the island (Fig. 3; Fig. 4, Appendix 1). To the SE, the volcanoclastic
413 deposits of the CPG are topped by the lacustrine limestones of Christian Hill that
414 contain feldspar and quartzitic debris (Fig. 3; Fig. 4). We interpret the volcanoclastic
415 series as deposited in an alluvial plain system with lakes (where the limestones
416 formed) and ephemeral braided alluvial fans (cf. Nemec and Steel, 1984) that was
417 located at the foot of a volcanic edifice located to the SW and corresponding
418 nowadays to the Basal Volcanic Suite. Volcanic activity during deposition of the CPG
419 was ongoing, as recorded by tuffites and lapilli-rich deposits. We mapped
420 discontinuous exposures of a tuffite member that is bright green in color and easy to
421 recognize in the field, which we use as a marker in our cross section (Fig. 3; Fig. 4,
422 Appendix 1). The CPG is overall a monoclinial succession striking ~ NW-SE and

423 dipping 10° toward the NE (Fig. 3). In the vicinity of normal faults, dips vary and
424 may be up to 30° (Fig. 3).

425 Previous maps (Martin-Kaye, 1969; Christman, 1973) suggested that the CPG
426 is overlying the BVS, but we carefully studied the contacts and did not find this
427 relationship: rather, the CPG is interfingering with the BVS, as a syn-magmatic
428 sedimentary sequence adjacent to the main volcanic edifice. This is supported by the
429 presence of volcanoclastic deposits within the CPG at Willoughby, Pigeon beach and
430 Galleon (Fig. 3, Fig. 4). At Nelson Dockyard, the volcanoclastic and green tuffite
431 layers of the CPG are intruded by mafic dykes (Fig. 5A) that follow a NW-SE
432 trending normal fault (Fig. 5B). From the NE-SW cross-section (Fig. 3), we estimate
433 a minimum thickness of 200 m for the CPG, but the true thickness may be much
434 thicker as the base of the sequence is not exposed.

435

436 Antigua Formation

437 At Galleon, Pigeon Beach, Five Island, Fort James, and Seaforth, patches of few
438 meter-thick, reefal limestones are observed resting either above the CPG or the BVS
439 (Fig. 3, Fig. 4). Previous authors (e.g., Thomas, 1942, Martin-Kaye, 1969, Bouysse
440 and Westercamp, 1983) interpreted these as interbedded in the CPG, but our
441 observations rather show that these patches are always unconformably overlying the
442 CPG and preserved in the hanging walls of normal faults. From microfacies analyses,
443 we dated these marine limestones from Zones P20 (Rupelian, 30.3-29.2 Ma) to P21b-
444 P22 (Chattian, 28.1-23 Ma).

445 The Antigua Fm. is exposed in the east of the island, upon the CPG. Local
446 observations (St-John, Fig. 6A) and the regional shallower monoclinical orientation
447 striking N140° and dipping 5° toward NE indicate an angular unconformity between

448 the CPG and the Antigua Fm (Fig. 3). The minimum thickness of the Antigua
449 formation is 80m and is estimated from section logging in Burma Quarry (Fig.4,
450 Appendix 1). From the cross-section (Fig. 3), we re-evaluate its thickness to 160m.
451 Centimeter-size sub-horizontal stylolite are observed within the top beds of the
452 Antigua Fm. (Fig. 3, Fig. 6B and 6C, Fig. 8) showing that the thickness of the
453 Antigua Fm. must have been perhaps some several hundred meters thicker, but the
454 overburden was later removed.

455 In the northwestern part of the island, the formation comprises: ~10 m- thick
456 coarse-grained cross bedded siliciclastic carbonates; 18 m-thick foraminiferal
457 packstones dated from Zones P18-P21a (Rupelian, 33.9-28.1 Ma) to P21b (Chattian,
458 28.1-26.8 Ma); 45 m thick coral biostromes (Fig. 6E) and foraminiferal wackestones
459 to packstones, dated to Zones P21 to P22 (upper Rupelian-Chattian) in their
460 lowermost part (Fig. 4, Fig. 10, Appendix 1 and 2). In the central part of the island the
461 Antigua Fm. comprises, from bottom to top: ~10 m-thick coarse grained mixed
462 carbonate and volcanoclastic grainstone with corals, dating from zones P18 to P21a
463 (Rupelian, 33.9-28.1Ma); 8m- thick foraminiferal wackestones and coral beds dating
464 from zones P21b to P22 (upper Rupelian-Chattian, 29.2-23 Ma); 5.5 m- thick
465 planktonic foraminiferal wackestones dating from zones P21b – P22 (Chattian) to
466 P22b-N4 (upper Chattian-Aquitania, 24-21 Ma) in the uppermost part (Fig. 4, Fig.
467 10, Appendix 2 and 3). The southeastern part of the Antigua Fm is made of few
468 meter-thick foraminiferal wackestones dated to Zones P18-P21a (Rupelian, 33.9-29.2
469 Ma) (Half Moon Bay) or Zones P22-N4 (upper Chattian-Aquitania, 26.8-21 Ma)
470 (Devil's Bridge) (Fig. 3, Fig. 4, Fig. 10, Appendix 1 and 2). The presence of several
471 interbedded mixed volcanoclastic-carbonate rocks indicates occasional mass flow
472 deposition.

473 The Antigua Fm was deposited in low angle reefal carbonate ramp setting
474 above the BVS and the CPG (Fig. 10). The sequence is composed of inner ramp coral
475 biostromal beds (Fig. 6E) changing southeastwards into planktonic foraminifera-rich
476 wackestones. An upward deepening trend is also recorded from reefal deposits in the
477 lower part of the formation to muddy, mid to outer ramp deposits in its uppermost
478 part. Our biostratigraphic constrains show that the Antigua Fm was deposited from
479 the late Rupelian (Zone P20, 30.3-29.2 Ma) to the late Chattian-Aquitanian (Zones
480 P22-N4, 26.8-21 Ma) (Fig. 10, Appendix 2).

481 The Antigua Fm includes reworked and weathered volcanoclastic beds that we
482 interpreted as turbidites or tempestites (Fig.4, Appendix 1) but nowhere did we find
483 volcanic ash or pumice deposits interbedded in the Antigua formation.

484

485 **Structure and kinematics of Antigua**

486 Mapped and outcrop-scale faults are normal faults that may be roughly
487 subdivided into three clusters: $\sim N020^\circ (\pm 020^\circ)$, $N090^\circ$ and $\sim N140^\circ (\pm 020^\circ)$. The fault
488 planes dips on average about 60° and show dip-slip slickenslides and displacements
489 up to tens of meters (Fig. 7). The $N020^\circ$ and $N090^\circ$ faults are observed in the three
490 units of Antigua but the $N140^\circ$ faults are absent in the Antigua Fm. The CPG and
491 Antigua Fm strike parallel to the $N140^\circ$ faults suggesting that these faults are
492 responsible for the main orientation of the island's stratigraphy. The trend of
493 Antiguan coastlines is controlled by each of these three fault populations: the
494 northwestern and south-eastern shores are trending NE-SW, the southern shore is E-
495 W trending and the northeastern and southwestern shore display a series of NW-SE
496 trending deep and narrow bays and capes. Although no direct crosscutting evidence
497 has been found in the field, at map scale the $N20^\circ$ faults seem to intersect the $N90^\circ$

498 and N140° faults, especially to the north of Liberta Hill and Christian Hill and on the
499 southeastern and northwestern coasts (Fig. 3). The N090° and N140° faults are well
500 visible in the CPG where they shape the landscape with the footwall consisting of
501 100- 200 m high hills that trend NW-SE (Christian Hill, All Saint Hill, Fig. 3).

502 At site scale, paleo-stress tensors indicate pure to radial extension with the
503 direction of stretching varying from NNW-SSE to E-W. Strike-slip faults were
504 observed only at one site (Old Road, Fig. 9A). Some sites display slightly oblique-slip
505 normal faulting (Fig. 9A). Evidence for syn-sedimentary activity was observed for
506 N090° faults at Fort James (injectites, Fig. 7A) and at Newfield (abrupt facies
507 changes and reworked reefal blocks across the fault, Fig. 6B). At Nelson Dockyard, a
508 N140° trending fault was intruded by a mafic dyke that we dated to 27.03 ± 1.89
509 (ANT20.12), giving a minimum fault age.

510 As the N020° and N090° faults are observed in the three units of Antigua but
511 the N140° faults are absent in the Antigua Fm, we assume that N20° and N90° faults
512 postdate N140° faults. Moreover, there is no clear cross cutting relationships between
513 N020° and N090° fault suggesting that they might be synchronous, therefore while
514 performing the kinematics inversion, we split our dataset separating N140° trending
515 faults from the N020°-N090° dataset, according to our field constraints and
516 observations. For the N140° faults set, we obtained a paleo-tensor with $\sigma_1 =$
517 N255°/80°, $\sigma_2 =$ N120°/0°, $\sigma_3 =$ N020°/10°, indicating that these faults
518 accommodated a NNE-SSW stretching (Fig. 9C). The paleo-tensors obtained for the
519 E-W and N-S trending faults show a subvertical σ_1 , a sub-horizontal N130°-trending
520 σ_2 , and a sub-horizontal, N030° trending σ_3 indicating NNE-SSW stretching (Fig.
521 9C). Due to the limited number of observed faults and lack of kinematics indicators
522 on fault planes, the quality of the tensors is poor (i.e., class D). Nonetheless, the

523 obtained tensors provide no evidence for major changes in the stress field during
524 deposition of the Antigua Fm: strain is minor, and characterized by a NNE-SSW
525 stretching direction that did not vary much during the Oligocene (Fig. 9C).

526

527 **Anisotropy of the magnetic susceptibility (AMS)**

528 Site mean susceptibility (k_m) of sites in the CPG ($31.31-76.55 \times 10^{-4}$ SI) and in
529 Antigua Fm ($0.052-25.59 \times 10^{-4}$) are indicative of a significantly high concentration
530 of ferromagnetic minerals. Corrected anisotropy degrees are low ($P' < 1.06$) with
531 values ranging from 1.014 to 1.058, suggesting a relatively weak tectonic overprint
532 (Table 3). The shape of AMS ellipsoid varies from oblate ($T > 0, F > L$) to triaxial (T
533 $\approx 0, F \approx L$) with a dominance of oblate ellipsoids, indicating that the tectonic fabric
534 has only partially overprinted the original sedimentary fabric (Borradaile and Jackson,
535 2004) (Table 3). Pure sedimentary fabrics are recognized at sites CH, TU1, CO and
536 PA, where k_{int} and k_{max} are randomly distributed within a plane sub-parallel to the
537 stratification (Fig. 9B). Tectonic fabrics are recognized at sites TU2, FJ, FI and DB,
538 where a well-defined (i.e., $e_{12} < 30^\circ$) magnetic lineation is observed (Fig. 9B, Table
539 3). This magnetic lineation is sub-horizontal to shallowly plunging towards NNE to
540 NE (Fig. 9B). This direction is sub-parallel to the regional NNE-SSW stretching
541 direction estimated from the fault kinematic analysis from the Basal Volcanic Suite,
542 the Central Plain Group and the Antigua Fm. (Fig.9C).

543

544 **DISCUSSION**

545 **Geological evolution of Antigua**

546 *Late Eocene - early Oligocene magmatic activity*

547 With a combination of field observations, lithostratigraphy, biostratigraphy,
548 and $^{40}\text{Ar}/^{39}\text{Ar}$ dating we establish the duration of magmatic activity in Antigua and
549 subsequent sedimentation. The lithostratigraphy of Antigua shows that magmatism
550 formed the Basal Volcanic Suite, and was active during the deposition of the
551 volcanoclastic Central Plain Group, but not during the deposition of the Antigua Fm
552 (Fig. 3). The stratigraphically lowest (tuffites) and highest (lacustrine limestones with
553 volcanic debris) units of the CPG that we observed in the field contain evidence of
554 explosive volcanism (Appendix 1). In the Antigua Fm. all volcanic elements are
555 reworked as clastic sediment but no evidence for explosive (ash deposits or pumice)
556 or effusive volcanism (intercalated lavas) was observed (Fig. 8B, Appendix 1). Our
557 field observations corroborate seismic interpretations of lines offshore Antigua, where
558 in megasequences interpreted to reflect the Oligocene and Neogene deposits, no
559 magmatic features (conic shaped bumps) were identified (Cornée et al., 2021; Fig. 11,
560 Appendix 3).

561 From our $^{40}\text{Ar}/^{39}\text{Ar}$ ages of a rhyolitic dyke (sample DWB-B) and a dacitic
562 dome (sample ANT 6.8) crosscutting the andesite-pyroclastic suite (35.32 ± 0.16 Ma
563 and 29.76 ± 0.22 Ma, respectively; Fig.7, Table 2), and the K/Ar age of Nagle et al.
564 (1976) of an andesitic lava (38.5 ± 2 Ma, Fig. 1, Table 1), we infer that the bulk
565 andesitic and explosive volcanism of the Basal Volcanic Suite occurred in the late
566 Eocene.

567 We discarded our age of 18.57 ± 1.26 Ma for the andesite from the BVS
568 (sample ANT 20.4) because it is inconsistent with the one of the rhyolitic dyke that
569 crosscut it. We assume that this sample was fully reset during a late (post-magmatic)
570 hydrothermal event as exemplified by the very high atmospheric contamination
571 within it. This is supported by the occurrence of various degrees of sub-greenschist

572 hydrothermal alteration within the Basal Volcanic Suite (albitized plagioclases,
573 chloritized orthopyroxenes and groundmass; Gunn and Roobol, 1976), the Central
574 Plain Group (chloritised tuffites; Jackson et al., 2013) and the Antigua Fm (silicified
575 limestones; Strang et al., 2018). Such pervasive subgreenschist hydrothermal
576 metamorphism has been described within the recent arc in the Guadeloupe and may
577 take place at 1 to 3-4 km depth (Favier et al., 2019).

578 Late volcanic activity occurred in Antigua at the transition between early and
579 late Oligocene and is exemplified by the emplacement of a dacitic dome through the
580 BVS and basaltic andesite dykes through the CPG and the Antigua Fm. The dacitic
581 dome yields a late Rupelian age of 29.76 ± 0.22 Ma (ANT 6.8, Sugar Hill). The mafic
582 dykes intruding the base of the Antigua Fm gives an age of 30.50 ± 0.70 Ma (ANT
583 20.6) that is consistent with the biostratigraphic dating to the late Rupelian (Zone P20,
584 30.3-29.2 Ma). As the CPG is synchronous with magmatic activity of the BVS and
585 capped by the Antigua Fm its age must range from at least 38 to 30 Ma (late
586 Bartonian to late Rupelian). The 27.03 ± 1.89 Ma age of a dyke crosscutting the CPG
587 is the youngest evidence for magmatic activity on Antigua (Fig. 5A, 5B).

588 The quartz diorite stock, now exposed at Old Road, gives only a minimum age of 28
589 Ma, and could represent a late-stage intrusion (ANT 20.8, Fig. 7, Table 2).

590

591 *Late Oligocene – early Miocene carbonate platform*

592 Following the end of magmatic activity, we observe a change from terrestrial
593 (CPG) to marine environment (Antigua Fm.) during the Rupelian-Chatian transition.
594 The depositional environment of the Antigua Fm. varies both geographically from
595 inner ramp coral biostromal beds (Fig. 6E) to the north-west to planktonic
596 foraminifera-rich wackestones to the south-east and temporally with reefal deposits in

597 the lower Rupelian part of the sequence to muddy, mid to outer ramp deposits in its
598 uppermost part (late Chattian to Aquitanian). We reinterpreted the marine carbonates
599 deposits, previously described as interbedded within the CPG (Masclé and
600 Westercamp, 1983), as residual exposures of the Rupelian lower part of the Antigua
601 Fm, preserved in grabens. This indicates that the Antigua Fm was entirely covering
602 the CPG and, consequently, that a transgressive event occurred in Antigua during the
603 P20 Zone (30.3-29.2 Ma, Rupelian). The late Rupelian-Chattian global sea level
604 variations (tens of meters; Miller et al., 2020) are smaller than those of the
605 depositional environment of the Antigua Fm (tens to hundreds of meters).
606 Consequently, we infer that the Island subsided during the late Rupelian–Chattian
607 interval. Thermal subsidence upon cooling after magmatic activity could have played
608 a role (Moore, 1970; Tallarico et al. 2003).

609 To account for the presence of centimetres long, subvertical pressure-
610 dissolution stylolitic peaks (Fig. 6C, 6D) the Antigua Fm must have undergone vertical
611 compaction related to a post-Aquitanian sedimentary pile that was later eroded. In the
612 neighbouring volcanic area, this erosional event and associated exhumation is
613 supported by the outcropping of sub-greenschist facies units, that are thought to be
614 originated from 1 to 3-4 km depth (Favier et al., 2019). In the offshore domain, the
615 megasequence 4 (MS4, Oligocene to Early Middle Miocene in Cornée et al., 2021),
616 that can be correlated to CPG and Antigua Fm, is topped by a major erosive Sequence
617 Boundary (SB5) dated as early middle- Miocene (Fig. 11, Appendix 3) and
618 recognized regionally (Cornée et al., 2021; Boucard et al., 2021). We thus suggest
619 that erosion occurred during early–middle Miocene time. After this period, the island
620 likely remained above sea-level as no post-Aquitanian sediments (aside from
621 Quaternary alluvium) can be observed. Meanwhile, the Willoughby Basin subsided

622 along the N090° faults bounding the Antigua bank to the South (Fig. 11). This stable
623 position appears consistent with the slow cooling estimated with QTQt modelling of
624 $^{40}\text{Ar}/^{39}\text{Ar}$ spectrum of plagioclase from the quartz diorite (~5° per Ma; sample ANT
625 20.8, Fig. 8) since 25 Ma at least – a similar cooling rate was recently reported from
626 the granodioritic plutons of St Martin island (Noury et al., 2021).

627

628 *A 20 Ma long magmatic lull*

629 The geological history we unraveled from Antigua thus includes (1) a main
630 magmatic pulse occurred in Antigua during the late Eocene (continuing to at least 35
631 Ma), (2) magmatic activity continued mainly during the early Oligocene in the form
632 of late-stage dykes and plugs (30.5 to 27 Ma), (3) magmatic activity ceased during the
633 late Oligocene synchronously with a regional transgressive event and a subsidence of
634 the island leading to the development of a carbonate platform completely devoid of
635 evidence of volcanism; (4) an early–middle Miocene exhumation and uplift event
636 responsible for the removal of a part of the volcanic and sedimentary series after
637 which Antigua stayed emerged and stable.

638 From our new age model, we find that, in the northern Lesser Antilles, the
639 main activity of the Paleogene arc occurred between the late Eocene and the early
640 Oligocene and show that magmatism – previously supposed to possibly continue into
641 the Miocene based on K-Ar ages (Nagle et al., 1976; Briden et al., 1979) – waned and
642 came to an arrest by ~27 Ma in Antigua. Small-volume, late-stage magmatism on
643 nearby islands St-Martin (24.4 Ma; Cornée et al., 2021) and St-Barthélemy (24.5 Ma;
644 Legendre et al., 2018) continued slightly longer. The recent arc, located further west
645 in the island of Saba, St-Kitts, Monserrat and Guadeloupe, is active since the
646 Pliocene. Our analysis thus supports a long magmatic lull in the northern Lesser

647 Antilles arc despite ongoing subduction at more or less constant rates (Leroy et al.,
648 2000; Boschman et al., 2014). With our new age model that includes $^{40}\text{Ar}/^{39}\text{Ar}$ dates
649 and lithostratigraphy, we more accurately constraining it to a *ca* 20 Ma period lasting
650 from the early late Oligocene to the Pliocene. As magmatic flareup contribute to
651 crustal thickening (Ma et al., 2022), the Paleogene activity of the Lesser Antilles arc
652 should have participated to the building of the GrANoLA land (Philippon et al.,
653 2020a), an emerged area that was spread out through the Northern Lesser Antilles to
654 Puerto Rico and favoured terrestrial fauna dispersal from South America to Greater
655 Antilles (e.g. Marivaux et al., 2020). The end of magmatic activity and subsequent
656 thermal and tectonic subsidence could have participated to the removal of this
657 pathway during late Oligocene. This is showing the importance of the understanding
658 of the magmatic history of the Lesser Antilles arc in the frame of paleo-(bio-
659)geographical history of the Eastern Caribbean region.

660

661 **A correlation between end of magmatism and tectonic changes ?**

662 In the Northern Lesser Antilles, a correlation between tectonics and
663 magmatism is suggested by the NW-SE orientation of the Paleogene arc that aligns
664 with the eastern flank of the NW-SE oriented Kalinago basin. This basin opened from
665 the Eocene to the late Oligocene, synchronously with magmatic activity (Cornée et
666 al., 2021).

667 At the scale of Antigua, we found evidences for syn-magmatic and syn-
668 sedimentary tectonic activity. Within the CPG, we estimate a pre- or Rupelian age for
669 the activity of a normal fault at Nelson Dockyard as it is intruded by a dyke dated at
670 27 Ma (this study). Furthermore, the presence of injectites at Fort James (Fig. 7A), of
671 abrupt facies changes and reworked reefal blocks in Newfield (Fig. 6B) and the NE

672 orientation of the magnetic lineation obtained from sites of the CPG and of the
673 Antigua Fm, that are consistent with the NE-SW stretching orientation obtained from
674 paleotensor, strongly suggest syn-sedimentary tectonic activity.

675 Synchronously with the arrest of magmatism, we observe a marine
676 transgression and a tilt of the Central Plain Group resulting in a 5° difference of the
677 mean dip beddings between the CPG and the Antigua Fm. This strongly suggests that
678 the late Rupelian-Chattian transgression reflects tectonic subsidence although thermal
679 subsidence could also have played a role. The gentle northeastward 5° dip of the
680 Antigua Fm and a general deepening of the paleo-environment toward the uppermost
681 part of the sequence indicate that the subsidence is active until at least early Miocene.

682 Our structural observations and AMS measurement does not show a clear
683 change in deformation behavior or directions during Oligocene. Both paleostress
684 tensors indicate a NNE-SSW directed stretching, which remained consistent over
685 time. In the BVS and CPG, this stress field is accommodated by dominant N140°
686 faults and N090° and N020° normal faults. In the Antigua Fm, N140° faults are not
687 recognized and the stress is accommodated by N090° and N020° faults. The absence
688 of N140° faults could be indicative of a lowering of the intensity of the deformation.
689 AMS results show that magnetic lineations acquired during syn-tectonic deposition
690 are consistent with the NNE-SSW stretching direction estimated by paleotensors. This
691 confirms that this stretching direction was dominant in Antigua from the early
692 Oligocene to the early Miocene even though different families of faults accommodate
693 it.

694 With our field and kinematic investigations, we did not see (1) significant
695 deformation in the Antigua Fm and (2) a change in stress field during the Oligocene.
696 The decrease or change in tectonic activity on the island is subtle and only outlined by

697 the absence of N140° faults in the Antigua Fm. Thus it is unlikely to correlate the end
698 of magmatism to a change in tectonic activity on Antigua.

699 On the island of St-Martin and St-Barthélemy, a switch from pure orthogonal-
700 to-the-trench to radial extension is recognized during the early Miocene (Legendre et
701 al., 2018; Noury et al., 2021). In the northern Lesser Antilles region, a change in
702 upper-plate deformation style from back arc rifting (Kalinago basin; Cornée et al.
703 2021) to fore-arc dissection (V-shape basin, Boucard et al., 2021) as well as drastic
704 vertical motion (Cornée et al., 2021; Boucard et al., 2021) is observed during the
705 Oligocene. Together with the arrest of magmatism, these changes in upper-plate
706 deformation and vertical motion are certainly controlled by subduction related
707 processes and slab parameters variations.

708

709 **What controls Lesser Antilles magmatic flare-ups and lull?**

710 The oldest volcanic rocks of the Lesser Antilles arc are ~42 Ma (Philippon et
711 al., 2020a), some 10 Ma younger than the NE-SW to E-W change in Caribbean-North
712 America plate motion that led to the to the formation of the modern day N-S trending
713 Lesser Antilles subduction zone (Briden et al., 1979; Boschmann et al , 2014).

714 Such a delay is often seen between the onset of subduction and the
715 development of a mature arc (e.g., Stern et al., 2012). During ~ 15 Ma (late Eocene to
716 late Oligocene), volcanic edifices developed on the eastern flank of the Kalinago
717 basin, and in this period, the arc-trench distance, and by inference, the slab angle,
718 remained more or less constant. But by the end of the Oligocene, magmatism ceased
719 in the Northern Lesser Antilles.

720 Several hypotheses have been proposed to explain this arrest. Bouysse and
721 Westercamp (1990) speculated that slab break-off occurred following the subduction

722 of a postulated buoyant, thick oceanic crust. But seismic tomographic images reveal a
723 continuous, non-broken slab reaching the mantle transition zone without evidence for
724 breaks (van Benthem et al., 2013; van der Meer et al., 2018; Braszus et al., 2021), and
725 the subduction rate has not changed (Boschmann et al., 2014). If a slab breakoff had
726 occurred, a new slab would have had to quickly formed to re-instate the arc as
727 observed.

728 Boucard et al., (2021) suggested that subduction erosion occurred during middle
729 Miocene time. Subduction erosion could push an arc towards the hinterland, but the
730 timing of this event (post-middle Miocene) cannot explain the late Oligocene onset of
731 the magmatic lull, and subduction erosion would migrate an arc, rather than stop its
732 activity.

733 Slab flattening is then a third option. Subduction of buoyant features (oceanic
734 aseismic ridges, oceanic plateaus, or seamount chains) is commonly thought to
735 possible trigger flat slab subduction at mantle-stationary trenches (Yang et al., 1996,
736 Gutscher et al., 2000; Gerya et al., 2009; Martinod et al., 2013, Ma et al., 2022). In the
737 Lesser Antilles region, McCann and Sykes (1984) were the first to propose that a
738 former anomalously thick aseismic ridge connecting the Barracuda ridge and the
739 Main Rise (Fig.1) and/or that fragments of the Bahamas platform interacted with the
740 subduction and could have triggered slab flattening and westward migration of the
741 volcanic center. To the North, the thin continental margin below the Bahamas bank
742 diachronously subducted and entered the Greater Antilles subduction zone Antilles in
743 the late Eocene after which subduction on Cuba ceased (Erikson et al., 1990; Mann et
744 al., 2002; Iturralde-Vinent et al., 2008; Granja-Bruna et al., 2010; Cruz-Orosa et al.,
745 2012; Lao-Davila et al., 2014). The eastern, ocean-ward end of the Bahamas bank
746 already interacted with the NE Caribbean margin during the Caribbean plate motion

747 change of the mid-Eocene and there is no clear reason to infer that this interaction
748 allowed for an arc in the late Eocene and early Oligocene, but not in the 20 Ma that
749 followed.

750 So while slab flattening may be a viable reason to explain the magmatic lull,
751 the obvious solutions inferring the arrival of buoyant features do not seem
752 straightforward solutions.

753 As showed by recent reconstructions of the Caribbean region, a change in the age of
754 the oceanic lithosphere subducted, from a young Proto-Caribbean oceanic crust to an
755 old America's oceanic crust is observed in the eastern Caribbean subduction zone
756 during the end of Oligocene (Braszus et al., 2021). Nevertheless, variation of the age
757 of the subducted oceanic lithosphere might not be by itself sufficient to change the
758 slab dip (Cruciani et al., 2005).

759 Schepers et al. (2017) showed for the Andean subduction zone that flat slabs may also
760 arise when roll-back of a subducted slab is locally impeded, and sub-slab mantle starts
761 to support a flat slab. But the Lesser Antilles trench can be considered more or less
762 stable relative to the mantle since 50 Ma following the kinematic reconstructions of
763 Boschmann et al. (2014) and roll-back was short-lived and restricted to the southern
764 portion of the trench, where the Grenada-Tobago Basin opened in the Eocene (Aitken
765 et al., 2011), before the magmatic lull. So the scenario for the Andes does not apply to
766 the Lesser Antilles arc.

767 We suggest that slab flattening in the northeastern corner of the Caribbean plate may
768 have originated from the progressive formation of the spoon-shaped, curved slab
769 (Laurencin et al., 2013; van Benthem et al., 2013; Braszus et al., 2021). The westward
770 motion of North America relative to the nearly mantle-stationary Caribbean plate
771 (Boschmann et al., 2014) and Lesser Antilles trench must be associated with

772 westward dragging of the south-dipping Puerto Rico part of the slab (Spakman et al.,
773 2018; van de Lagemaat et al., 2018; Parsons et al., 2021). With ongoing absolute
774 westward motion of North America, the E-W segment of the Puerto Rico segment
775 becomes longer (Boschmann et al., 2014), and in the curved area, the slab folds and
776 may flatten (Fig. 12). This curvature and flattening could have been minimal in the
777 Eocene, allowing for a regular volcanic arc, but became progressively more intense,
778 which may explain the long magmatic lull (Cerpa et al., 2021). We speculate that the
779 recent reinstatement of arc magmatism in the northern Lesser Antilles may relate to a
780 recently seismically imaged gap in the slab in the bend area (Meighan et al., 2013)
781 that may have allowed for the slab to steepen (Fig. 12).

782 Evaluating whether this may explain the Pliocene magmatic flareup requires
783 further dynamic and magmatic analysis and is beyond the scope of this paper. We
784 note, however, that if the magmatic lull is caused by slab flattening, the Pliocene
785 flareup may provide a proxy for reorganization in slab dynamics in the northeastern
786 Caribbean region. A detailed kinematic reconstruction of the northeastern Caribbean
787 plate boundary zone back to the onset of magmatism would be helpful to establish the
788 temporal and spatial relationships between subduction and the length of the E-W
789 trench segment east of Puerto Rico, and magmatism.

790

791 **CONCLUSION**

792 In this study, we revise the geological architecture and history of Antigua and
793 integrate our findings within the regional frame of both the Lesser Antilles arc
794 evolution and of the Caribbean upper plate strain pattern.

795 With lithostratigraphy, structural mapping, $^{40}\text{Ar}/^{39}\text{Ar}$ dating and
796 biostratigraphy, we revised the geological map of the island and provide a new age

797 model for magmatism and sedimentation of the island. The climax of magmatic
798 activity and concomitant volcanoclastic deposition emplaced during late Eocene and
799 continued until early Oligocene in the form of late-stage domes and dykes. From the
800 early Oligocene to, at least, the early Miocene, the island subsided along NW-SE
801 fault, resulting in subsequent transgression and deposition of a carbonate platform.
802 The island was then uplifted and partially eroded during the early-middle Miocene
803 and since that time, the island stayed emerged and stable. With a kinematic analysis
804 coupling paleotensors and anisotropy of the magnetic susceptibility (AMS), we show
805 that minor normal faulting accommodates NE-SW stretching and that, at island-scale,
806 there is not a clear change in deformation style that accompanies the end of
807 magmatism during Oligocene.

808 This integrative geological study of Antigua restricts the period of magmatic
809 activity on this island and definitively confirms the existence of a 20 Ma-long
810 magmatic lull in the northern Lesser Antilles. The Paleogene arc that is also
811 recognized in St-Martin and St-Barthélemy was emplaced along the eastern flank
812 Kalinago basin, synchronously with its rifting. The concordance in the period of
813 magmatic activity and of the occurrence of a large emerged area in the Lesser Antilles
814 (GrANoLA land) suggests that the magmatic evolution of the Lesser Antilles arc
815 could have participated to terrestrial pathways building and demise with crustal
816 thickening during flareups and thermal subsidence during lull.

817 During the Oligocene, magmatism ceased contemporaneously with a change
818 in upper-plate deformation from back-arc, perpendicular to the trench stretching
819 (Kalinago basin) to fore-arc, parallel to the trench stretching (V-shaped basins). This
820 episode is followed by regional uplift during early-middle Miocene. We postulate that
821 the end of magmatic activity, the change in upper-plate deformation style and vertical

822 motion may have been triggered by slab flattening originated from the progressive
823 formation of the spoon-shaped, curved slab. Nevertheless, this is still hypothetical and
824 further constrains on the kinematic evolution of the northeastern Caribbean plate
825 boundary back to Eocene are needed to understand the relation between magmatism,
826 upper-plate deformation and subduction.

827

828 **ACKNOWLEDGMENTS**

829 The authors would like to warmly thank Arthur Iemmolo of the University of
830 Montpellier for its precious help in $^{40}\text{Ar}/^{39}\text{Ar}$ analyses and and Fabienne Zami of the
831 University of Antilles and Christophe Nevado of the University of Montpellier for the
832 thin sections. A special thank to the National park of Antigua and especially to Dr.
833 Reg Murphy and to Chris Waters that allowed us the access to special sites and
834 accompagnied us in the field. This work was supported by the GAARAnti project
835 (ANR-17-31 CE-0009) and by the INSU TelluS-SYSTER grant call 2017-2019.
836 DJJvH acknowledges Netherlands Organization for Scientific Research (NWO) Vici
837 grant 865.17.001.

838

839

840

841

842

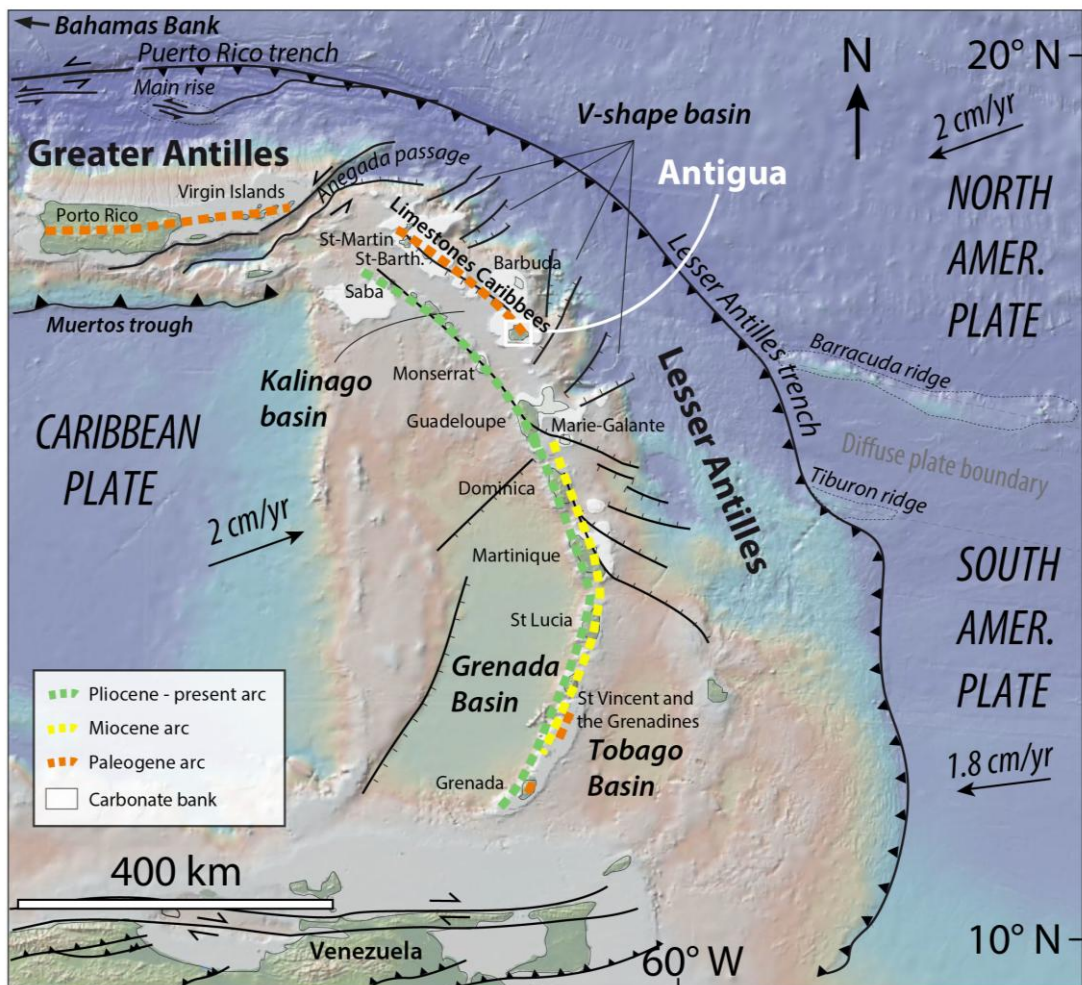
843

844

845

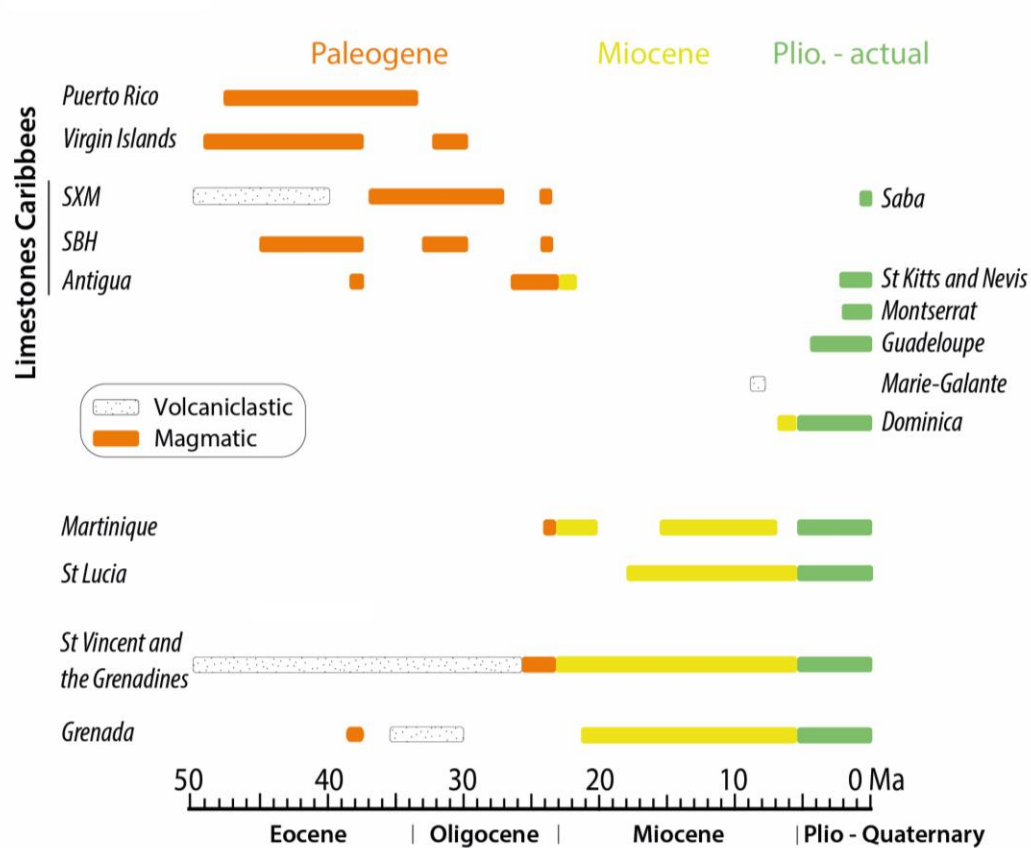
846

847 **FIGURE**



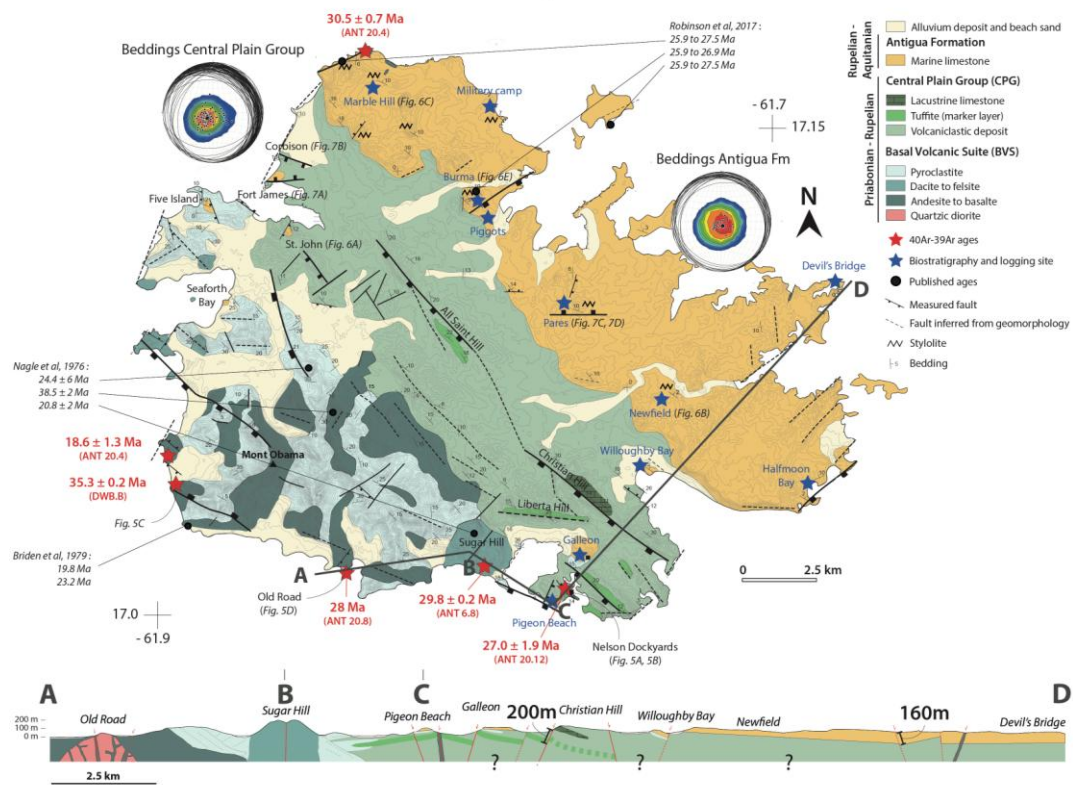
848

849 Figure 1. Bathymetric map, tectonic and volcanic settings of the Lesser Antilles
 850 subduction zone. The main faults are drawn from Cornée et al. (2021). The study area
 851 (Antigua) is outlined by the white square. Velocity vectors of the Caribbean and
 852 North and South Americas plates are from Symithe et al., 2015.



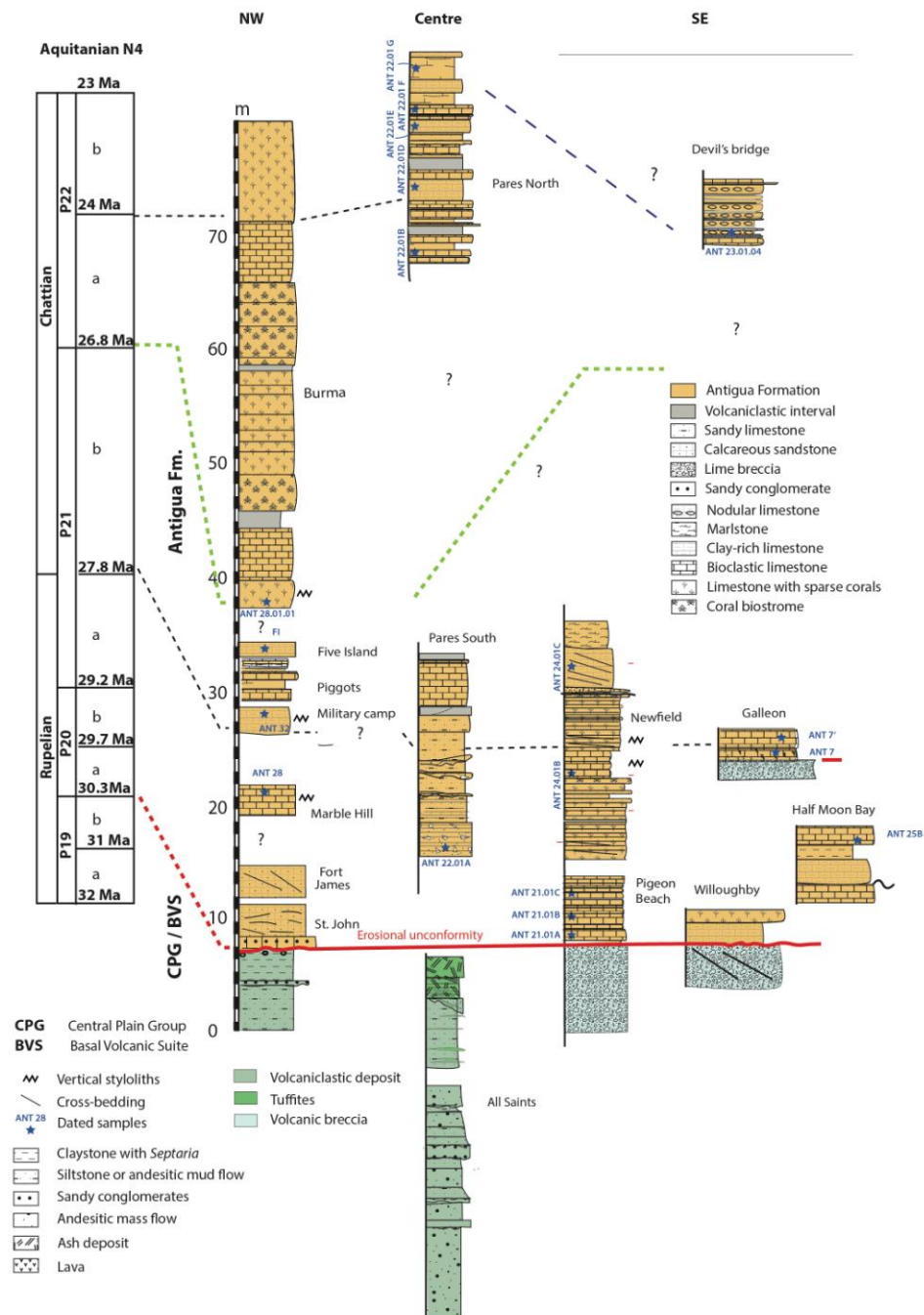
853

854 Figure 2. Schematic representation of the dated magmatic and volcanoclastic onshore
 855 evidences of the Lesser Antilles arc, from Eocene to present. The references used for
 856 the construction of this sketch are presented in Table 1.



857

858 Figure 3: Revised geological map and synthetic cross-section of Antigua. The map
 859 was constructed based on the map of Martin-Kaye (1959, 1969) and Christman
 860 (1973), and completed and updated with fieldwork observations, lithostratigraphy and
 861 structural measurements. The cross-section is located by a grey line on the map. The
 862 tuffite layer (light green) was used as a marker layer in the construction of the cross-
 863 section. Beddings are plotted on lower hemisphere. The K-Ar ages (Nagle et al.,
 864 1976; Briden et al., 1979) and the Sr-Sr ages (Robinson et al., 2017) are represented
 865 in italic.



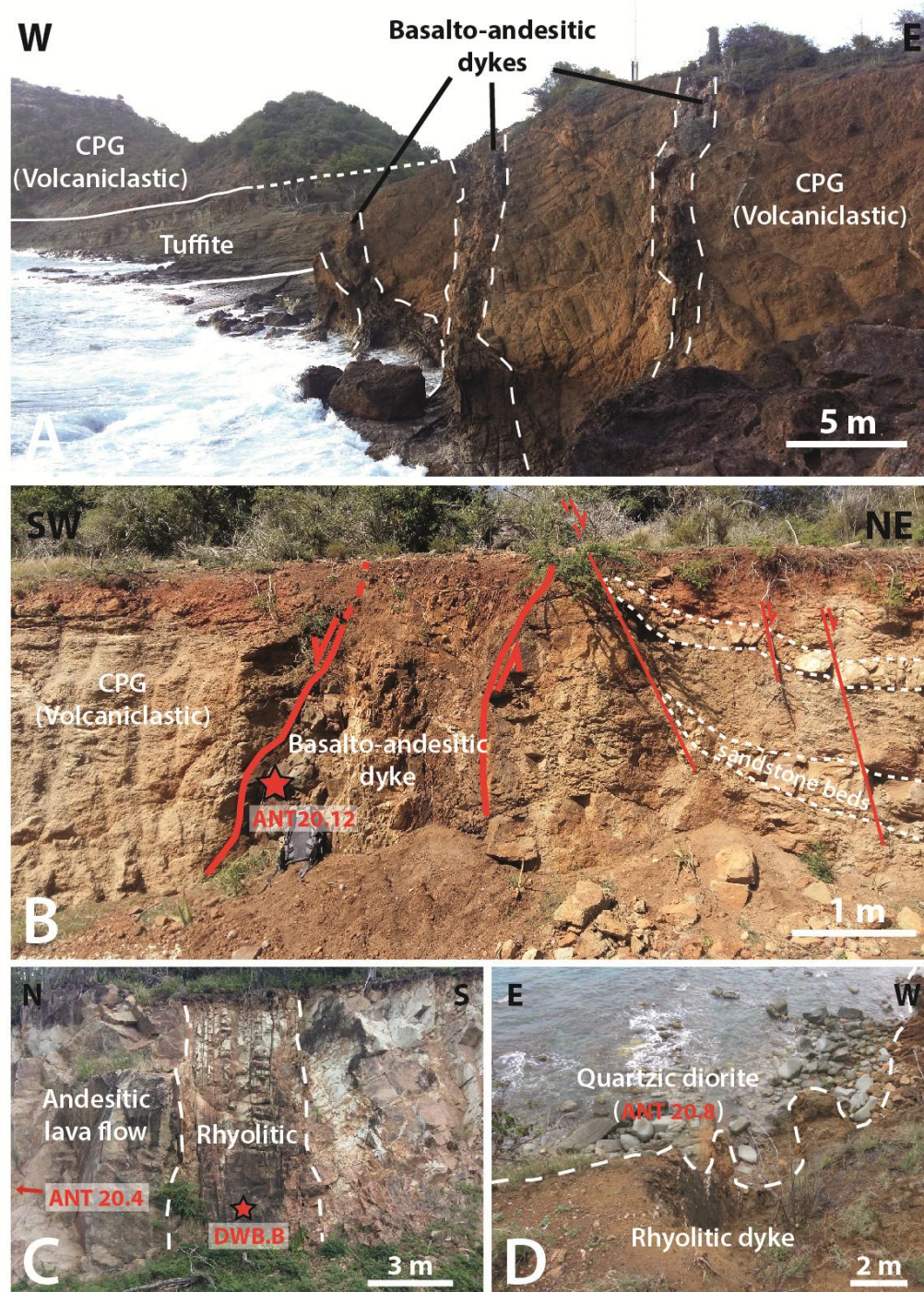
866

867 Figure 4. Stratigraphic synthesis and lithological successions of the Antiguan units.

868 The locations of the sections are presented in Fig.3. See Appendix 1 for a detailed

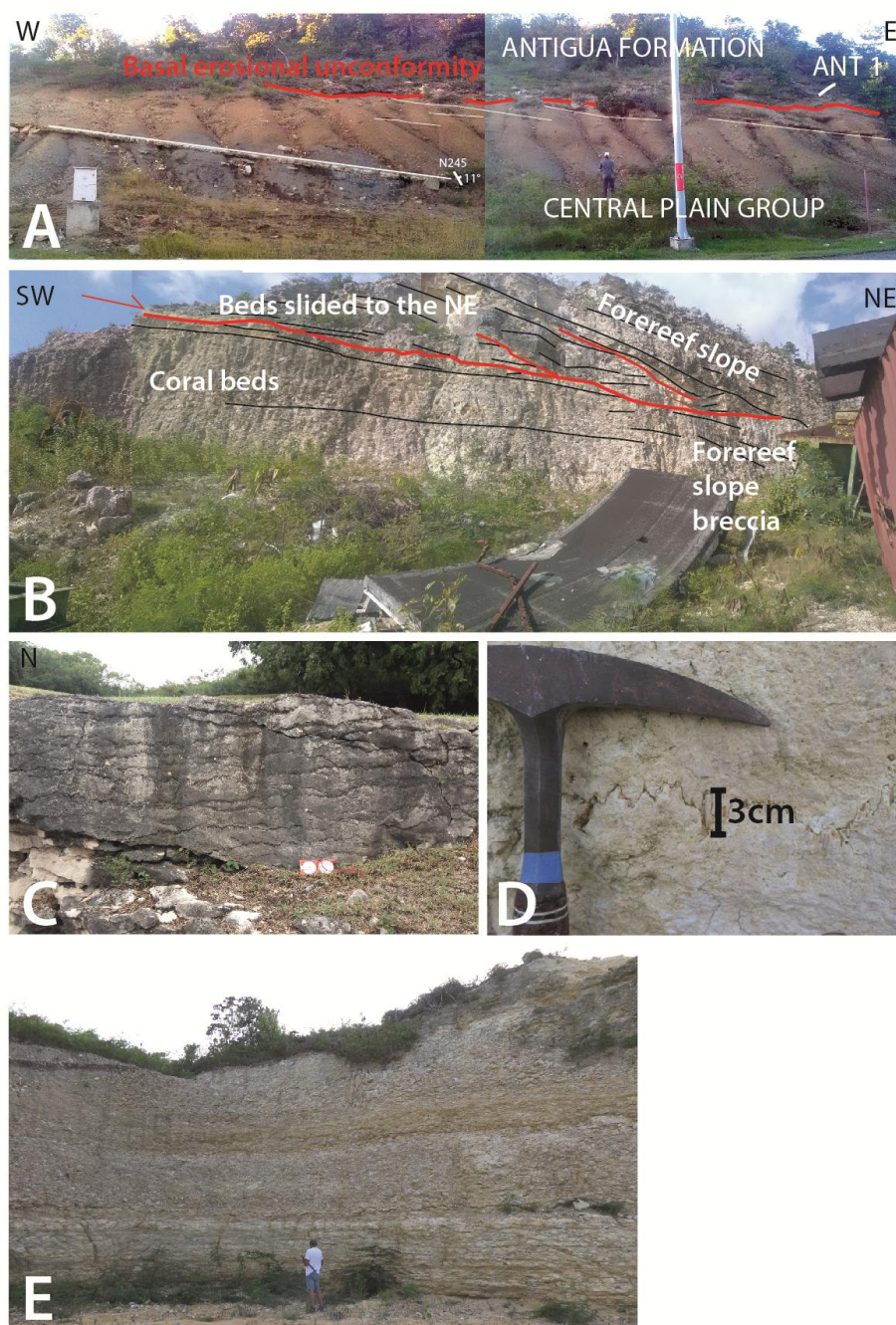
869 description of each sections.

870



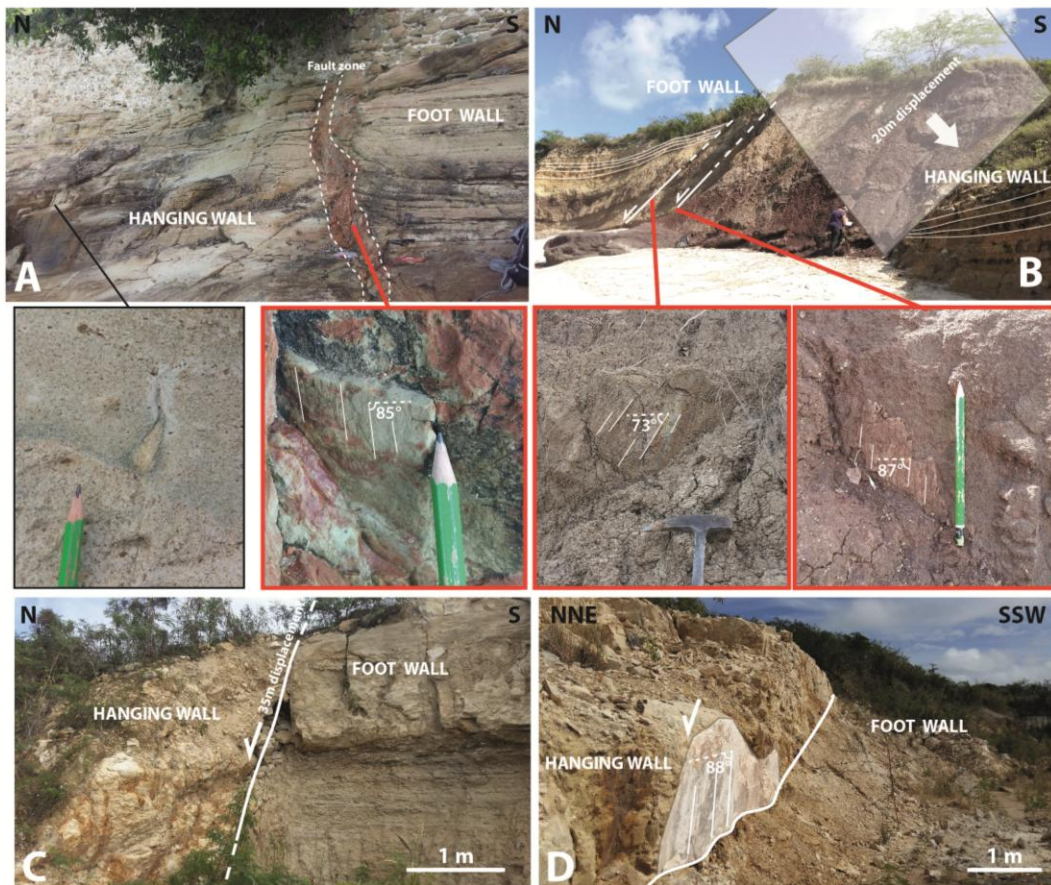
871

872 Figure 5. Field photography of the Basal Volcanic Suite and of the Central Plain
 873 Group. **A:** basaltic andesite dykes crosscutting the volcaniclastic deposits of the
 874 Central Plain Group; **B:** basaltic andesite dyke intruding a NW-SE trending normal
 875 faults and crosscutting the Central Plain Group; **C:** 35 Ma- old rhyolitic dyke (Sample
 876 DWB-B) crosscutting an andesite lava flow; **D:** quartzitic diorite stock crosscut by a
 877 rhyolitic dyke.



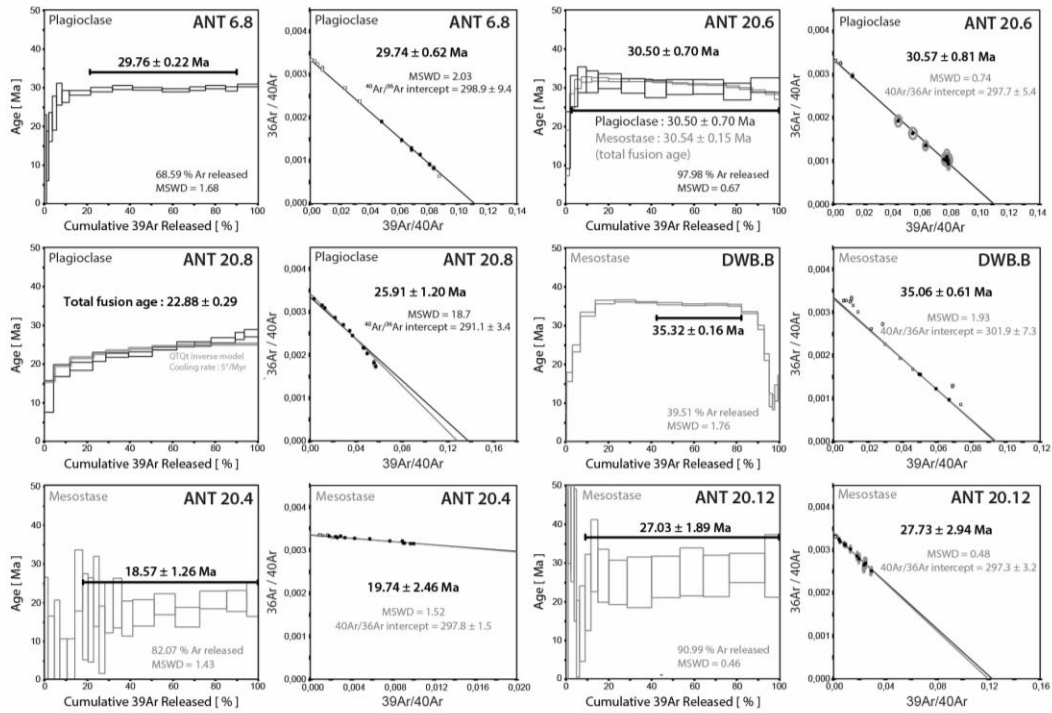
878

879 Figure 6. Field photography of the sedimentary units of Antigua. **A:** Unconformity
 880 between the Central Plain Group and the lower part of the Antigua Fm, observed at
 881 Saint-John. Cross-bedded conglomeratic limestones rest above tilted and eroded silty
 882 claystones of the CPG; **B:** abrupt change from reef platform to foreereef slope at
 883 Newfield Quarry. Note the presence of blocks slid towards the NE; **C:** wavy
 884 subhorizontal stylolitic surfaces in foraminiferal wackestones, Marble Hill. **D:** vertical
 885 stylolites at Burma Quarry; **E:** coral beds with diverse massive and platy coral
 886 colonies (upper part of the Burma Quarry). For location, see Fig.3.



887

888 Figure 7. Field photography of normal faults and associated high-angle striation at (A)
 889 Fort James, (B) Corbison beach and (C) and (D) Pares Quarry. Note the presence of
 890 injectites (sediment injection during earthquakes), representative of syn-sedimentary
 891 deformation at Fort James.



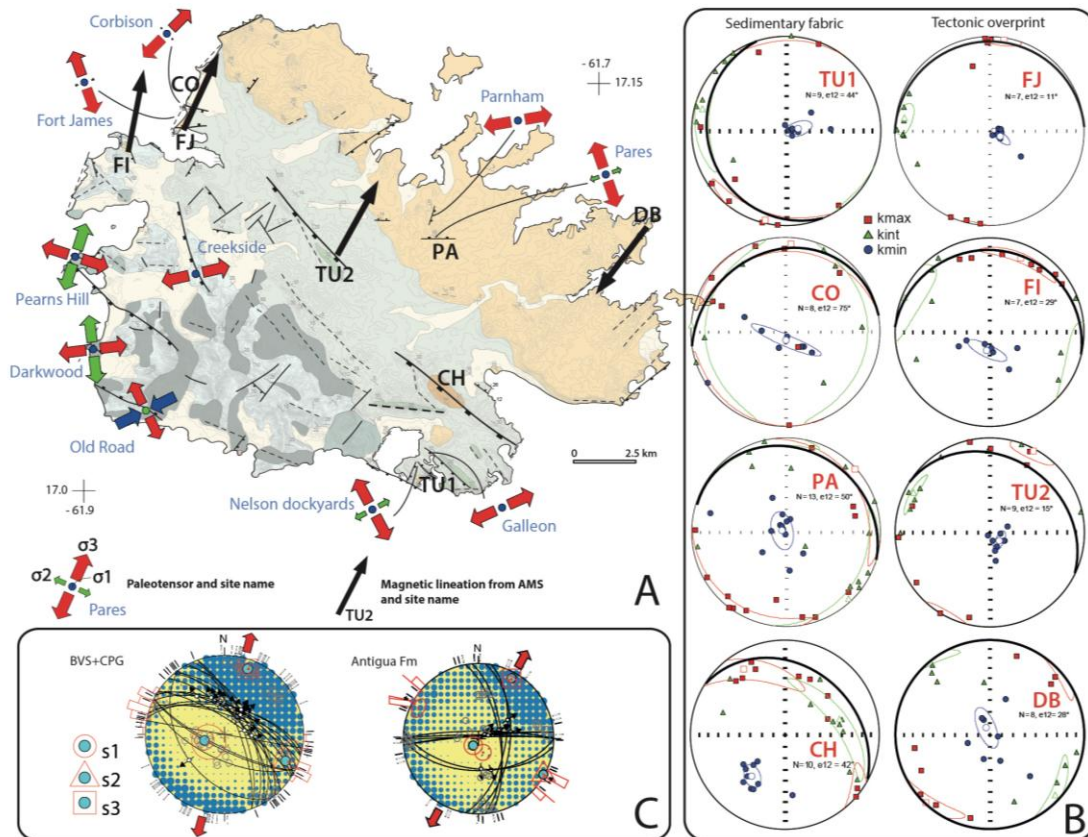
892

893 Figure 8 : $^{40}\text{Ar}/^{39}\text{Ar}$ spectra and inverse isochron for the samples from Antigua.

894 MSWD = mean square weighted deviation. The thick grey line in the spectra of ANT

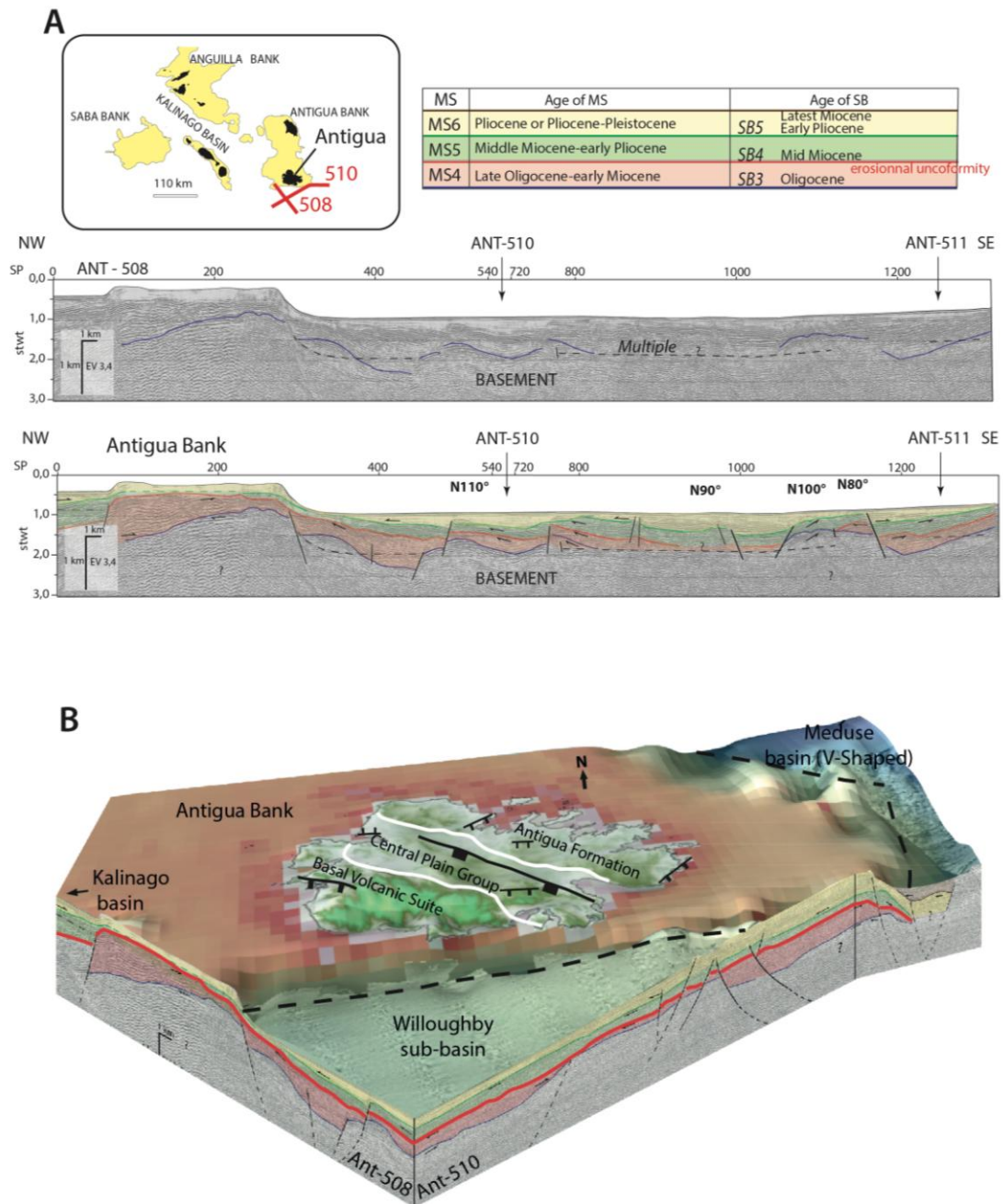
895 20.8 corresponds to the spectrum modeled using QTQt software (Gallagher, 2012).

896

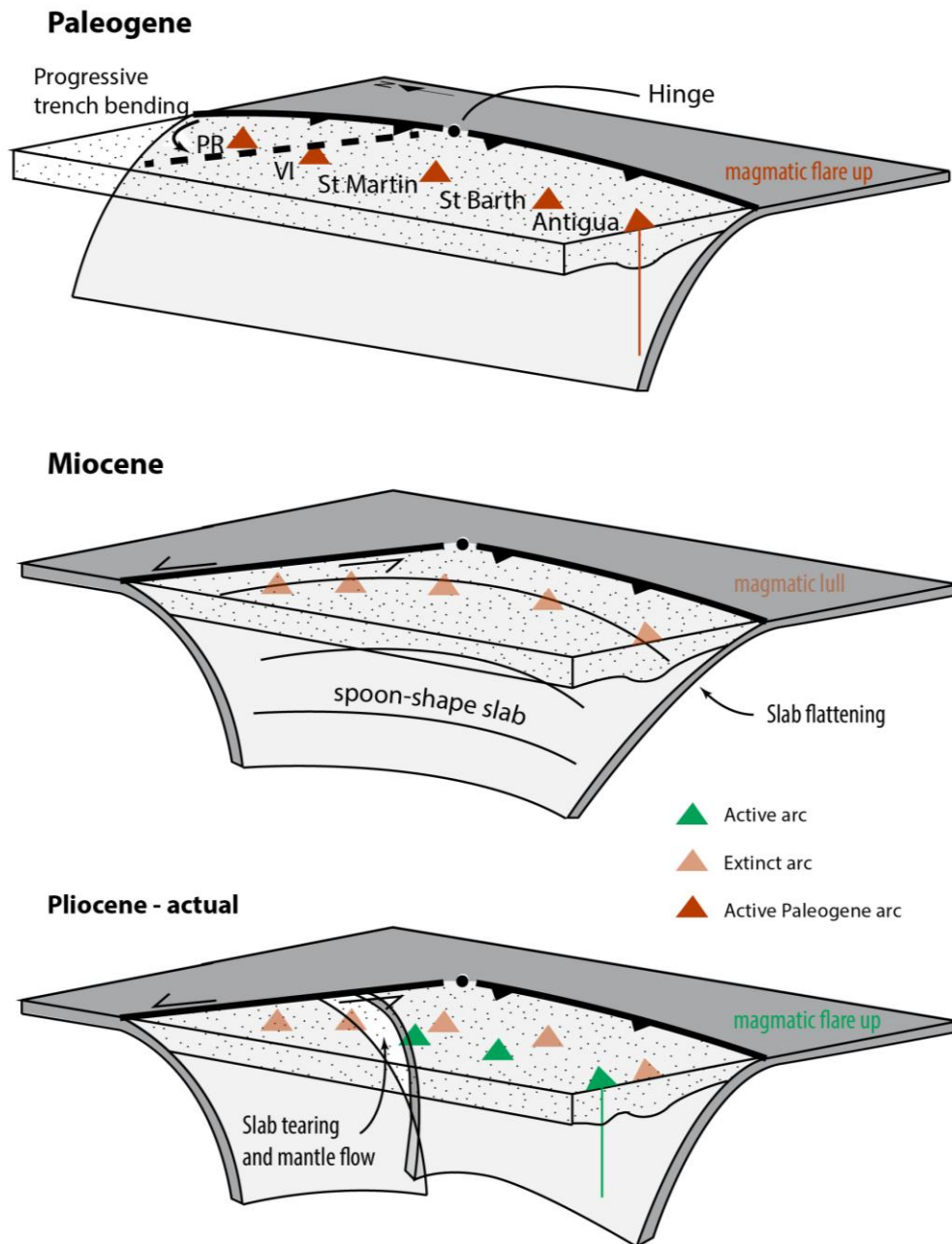


897

898 Figure 9 : **A:** Kinematic map of Antigua with paleotensors estimated per faults and
 899 magnetic lineation estimated from Anisotropy of the magnetic susceptibility (AMS)
 900 analysis; **B:** Schmidt equal area projections of the AMS ellipsoid principal axis for all
 901 sampled sites in geographic coordinates. 95% confidence ellipses and associated
 902 mean values for each axis are represented by coloured line and empty symbols
 903 respectively. Bold black arc represents the mean bedding plane of the site; **C:**
 904 Paleostress tensor obtained from the field data (faults with kinematic criteria and
 905 fractures) for the NW-SE trending faults within the Basal Volcanic Suite and the
 906 Central Plain Group (to the left) and for the E-W and N-S trending faults of the
 907 Antigua Formation (to the right).



915
 916 Figure 11. **A** : Time calibrated seismic stratigraphy analysis of the seismic profiles
 917 CPEM 508 and 510 (ARCANTE 3 Cruise, Bouysse et al., 1985a, 1985b; Bouysse
 918 and Masclé, 1994) from Cornée et al., 2021. Top: non interpreted; below : interpreted.
 919 The definition and time calibration follow the seismic stratigraphy chart defined by
 920 Cornée al. (2021) in the northeastern Lesser Antilles. MS: MegaSequence; SB:
 921 Sequence Boundary; **B** : 3D block with seismic profiles 508 and 510 showing the
 922 onshore and offshore structures in Antigua, Willoughby basin and the V-shaped
 923 Meduse basin. Note the erosional character of the SB4 unconformity that seals prior
 924 faults affecting MS4.



925

926 Figure 12 : Schematic 3D sketch of the progressive curvature of the Lesser Antilles

927 slab from Eocene to present and its impact on slab dip variation and magmatism

928 location.

929

930

931

932

933 **REFERENCES CITED**

- 934 Aitken, T., Mann, P., Escalona, A., & Christeson, G. L., 2011. Evolution of the Grenada and
935 Tobago basins and implications for arc migration. *Marine and Petroleum*
936 *Geology*, 28, 235-258. <https://doi.org/10.1016/j.marpetgeo.2009.10.003>
- 937 Alminas, H. V., Foord, E. E., Tucker, R. E., 1994, Geochemistry, mineralogy, and
938 geochronology of the US Virgin Islands, v. 2057. US Government Printing Office.
- 939 Andréïeff, P., Bouysse, P., Westercamp, D., 1987, Géologie de l'arc insulaire des Petites
940 Antilles, et évolution géodynamique de l'Est-Caraïbe, (PhD thesis), Université de
941 Bordeaux I.
- 942 Angelier, J., 1979, Determination of the mean principal directions of stresses for a given
943 fault population. *Tectonophysics*, v.56, no.3-4, p.17-26.
- 944 Baker, P. E., 1984., Geochemical evolution of St Kitts and Montserrat, Lesser Antilles.
945 *Journal of the Geological Society*, v.141, no.3, p.401-411
- 946 Blake, D.B., Donovan, S.K., Christopher L. Mah, C.L., Dixon, H.L., 2015, Asteroid
947 (Echinodermata) skeletal elements from upper Oligocene deposits of Jamaica and
948 Antigua. *Geological Magazine*, v.152, p. 1043–1056. [doi:10.1017/S0016756815000096](https://doi.org/10.1017/S0016756815000096)
- 949 Barabas, A.H., 1982, Potassium-argon dating of magmatic events and hydrothermal activity
950 associated with porphyry copper mineralization in west central Puerto Rico.
951 *Economic Geology*, v. 77, p. 109–126. <https://doi.org/10.2113/gsecongeo.77.1.109>
- 952 Borradaile, G.J., Jackson, M., 2004, Anisotropy of magnetic susceptibility (AMS): magnetic
953 petrofabrics of deformed rocks. Geological Society, London, Special Publications , v.
954 238, p. 299–360. <https://doi.org/10.1144/GSL.SP.2004.238.01.18>
- 955 Boschman, L.M., van Hinsbergen, D.J.J., Torsvik, T.H., Spakman, W., Pindell, J.L., 2014,
956 Kinematic reconstruction of the Caribbean region since the Early Jurassic. *Earth-*
957 *Science Reviews*, v.138, p. 102–136. <https://doi.org/10.1016/j.earscirev.2014.08.007>
- 958 Boucard, M., Marcaillou, B., Lebrun, J. - F., Laurencin, M., Klingelhofer, F., Laigle, M.,

- 959 Lallemand, S., Schenini, L., Graindorge, D., Cornée, J. - J., Münch, P., Philippon,
960 M., the ANTITHESIS and GARANTI Scientif, 2021, Paleogene V - Shaped Basins
961 and Neogene Subsidence of the Northern Lesser Antilles Forearc. Tectonics, v.40.
962 <https://doi.org/10.1029/2020TC006524>
- 963 BouDagher-Fadel, M. K. , 2015, Biostratigraphic and Geological Significance of Planktonic
964 Foraminifera (Updated 2nd Edition) London: UCL Press.
965 doi:10.14324/111.9781910634257
- 966 BouDagher-Fadel, M. K., 2018a, Evolution and Geological Significance of Larger Benthic
967 Foraminifera. London, UK: UCL Press. doi:10.14324/111.9781911576938
- 968 BouDagher-Fadel, M. K., 2018b, Revised diagnostic first and last occurrences of Mesozoic
969 and Cenozoic planktonic foraminifera. UCL Office of the Vice-Provost Research,
970 Professional Papers Series, p. 1-5.
- 971 Bouysse, P., Andréieff, P., Richard, M., Baubron, J. C., Mascle, A., 1985, Aves Swell and
972 northern Lesser Antilles Ridge: rock-dredging results from ARCANTE 3 cruise. In :
973 Symposium géodynamique des Caraïbes, p. 65-76, Technip Ed.
- 974 Bouysse, P., Westercamp, D., 1990, Subduction of Atlantic aseismic ridges and Late
975 Cenozoic evolution of the Lesser Antilles island arc. Tectonophysics, v 175, p. 349–
976 380. [https://doi.org/10.1016/0040-1951\(90\)90180-G](https://doi.org/10.1016/0040-1951(90)90180-G)
- 977 Bouysse, P., Mascle, A., 1994, Sedimentary basins and petroleum plays around the French
978 Antilles. In Hydrocarbon and Petroleum Geology of France, p. 431-443. Springer,
979 Berlin, Heidelberg.
- 980 Braszus, B., Goes, S., Allen, R., Rietbrock, A., Collier, J., Harmon, N., Henstock, T., Hicks,
981 S., Rychert, C.A., Maunder, B., van Hunen, J., Bie, L., Blundy, J., Cooper, G., Davy,
982 R., Kendall, J.M., Macpherson, C., Wilkinson, J., Wilson, M., 2021, Subduction
983 history of the Caribbean from upper-mantle seismic imaging and plate reconstruction.
984 Nat. Commun, v. 12, no. 4211. <https://doi.org/10.1038/s41467-021-24413-0>
- 985 Briden, J.C., Rex, D.C., Faller, A.M., Tomblin, J.F., 1979, K-Ar Geochronology and

- 986 Palaeomagnetism of Volcanic Rocks in the Lesser Antilles Island Arc. Philosophical
987 Transactions of the Royal Society of London. Series A, Mathematical and Physical
988 Sciences, v. 291, p. 485–528.
- 989 Brown, A.P., Pilsbry, H.A., 1914, Fresh-water mollusks of the Oligocene of Antigua.
990 Proceedings of the Academy of Natural Sciences of Philadelphia v. 66, p. 209-213.
- 991 Brown, G.M., Holland, J.G., Sigurdsson, H., Tomblin, J.F., Arculus, R.J., 1977,
992 Geochemistry of the Lesser Antilles volcanic island arc. *Geochimica et*
993 *Cosmochimica Acta* v. 41, p. 785–801. [https://doi.org/10.1016/0016-7037\(77\)90049-](https://doi.org/10.1016/0016-7037(77)90049-7)
994 [7](https://doi.org/10.1016/0016-7037(77)90049-7)
- 995 Cawood, P.A., Kröner, A., Collins, W.J., Kusky, T.M., Mooney, W.D., Windley, B.F., 2009,
996 Accretionary orogens through Earth history. Geological Society, London, Special
997 Publications, v.318, p. 1–36. <https://doi.org/10.1144/SP318.1>
- 998 Cerpa, N.G., Hassani, R., Arcay, D., Lallemand, S., Garrocq, C., Philippon, M., Cornée, J. -
999 J., Münch, P., Garel, F., Marcaillou, B., Mercier de Lépinay, B., Lebrun, J. - F.,
1000 2021. Caribbean Plate Boundaries Control on the Tectonic Duality in the Back- Arc
1001 of the Lesser Antilles Subduction Zone During the Eocene. *Tectonics* 40.
1002 <https://doi.org/10.1029/2021TC006885>
- 1003 Chadima, M., Hrouda, F., & Jelínek, V., 2020, Anisoft5. AGICO: Brno, Czech Republic.
- 1004 Miller et al, Cenozoic sea-level and cryospheric evolution from deep-sea geochemical
1005 and continental margin records, 2020. *SCIENCE ADVANCES* 16.
- 1006 Christman, R.A., 1973, Volcanic geology of southwestern Antigua, B.W.I. Geological
1007 Society of America Memoir, v.132, p. 439-448.
- 1008 Christeson, G.L., Mann, P., Escalona, A., and Aitken, T.J., 2008, Crustal structure of the
1009 Caribbean–northeastern South America arc-continent collision zone: *Journal of*
1010 *Geophysical Research–Solid Earth*, v. 113, no. B8, B08104, [https://doi](https://doi.org/10.1029/2007jb005373)
1011 [.org/10.1029/2007jb005373](https://doi.org/10.1029/2007jb005373).
- 1012 Cruciani, C., Carminati, E., Doglioni, C., 2005. Slab dip vs. lithosphere age: No direct

- 1013 function. Earth and Planetary Science Letters 238, 298–310.
1014 <https://doi.org/10.1016/j.epsl.2005.07.025>
- 1015 Cornée, J.-J., Münch, P., Philippon, M., BouDagher-Fadel, M., Quillévéré, F., Melinte-
1016 Dobrinescu, M., Lebrun, J.-F., Gay, A., Meyer, S., Montheil, L., Lallemand, S.,
1017 Marcaillou, B., Laurencin, M., Legendre, L., Garrocq, C., Boucard, M., Beslier, M.-
1018 O., Laigle, M., Schenini, L., Fabre, P.-H., Antoine, P.-O., Marivaux, L., 2021, Lost
1019 islands in the northern Lesser Antilles: possible milestones in the Cenozoic dispersal
1020 of terrestrial organisms between South-America and the Greater Antilles. Earth-
1021 Science Reviews, v.217, no. 103617. <https://doi.org/10.1016/j.earscirev.2021.103617>
- 1022 Cross, T.A., Pilger, R.H., 1982, Controls of subduction geometry, location of magmatic arcs,
1023 and tectonics of arc and back-arc regions. Geological Society of America Bulletin
1024 v.93, no.545. [https://doi.org/10.1130/0016-7606\(1982\)93<545:COGLO>2.0.CO;2](https://doi.org/10.1130/0016-7606(1982)93<545:COGLO>2.0.CO;2)
- 1025 Cruz-Orosa, I., Sàbat, F., Ramos, E., Vázquez-Taset, Y.M., 2012, Synorogenic basins of
1026 central Cuba and collision between the Caribbean and North American plates.
1027 International Geology Review, v.54, p.876–906.
1028 <https://doi.org/10.1080/00206814.2011.585031>
- 1029 Dagain, J., Andréiff, P., Westercamp, D., Bouysse, P., Garrabe, F., 1989, Notice et carte
1030 géologique de Saint-Martin 1/50 000, Antilles Françaises, Département de la
1031 Guadeloupe, v. 3). BRGM.
- 1032 Davidson, J. P., Boghossian, N. D., Wilson, M., 1993, The geochemistry of the igneous rock
1033 suite of St Martin, northern Lesser Antilles. Journal of Petrology, v.34, no.5, p.839-
1034 866
- 1035 Davies, J.H., Stevenson, D.J., 1992, Physical model of source region of subduction zone
1036 volcanics. Journal of. Geophysical Research, v.97, p.2037–2070.
1037 <https://doi.org/10.1029/91JB02571>
- 1038 Defant, M.J., Sherman, S., Maury, R.C., Bellon, H., de Boer, J., Davidson, J., Kepezhinskas,

- 1039 P., 2001, The geology, petrology, and petrogenesis of Saba Island, Lesser Antilles.
1040 Journal of Volcanology and Geothermal Research, v.107, p.87–111.
1041 [https://doi.org/10.1016/S0377-0273\(00\)00268-7](https://doi.org/10.1016/S0377-0273(00)00268-7)
- 1042 Delvaux, D., Sperner, B., 2003, New aspects of tectonic stress inversion with reference to the
1043 TENSOR program. Geological Society, London, Special Publications, v.212, p.75–
1044 100. <https://doi.org/10.1144/GSL.SP.2003.212.01.06>
- 1045 Donovan, S., Pickerill, R., Portell, R., Jackson, T., Harper, D., 2003. The Miocene
1046 palaeobathymetry and palaeoenvironments of Carriacou, the Grenadines, Lesser
1047 Antilles. Lethaia, v.36, p.255–272. <https://doi.org/10.1080/00241160310004666>
- 1048 Donovan, S. K., Jackson, T. A., Harper, D. A., Portell, R. W., and Renema W., 2014, The
1049 upper Oligocene of Antigua: the volcanic to limestone transition in a limestone
1050 Caribbee. Geology Today, v.30, p.151-158.
- 1051 Donovan, S.K., Harper, D.A.T., Portell, R.W. 2015, In deep water: a crinoid-brachiopod
1052 association in the Upper Oligocene of Antigua, West Indies. Lethaia 48, 291-298.
- 1053 Donovan, S.K., David A.T., Harper, D.A.T, Portell, R.W., Toomey, J.K., 2017, Echinoids as
1054 hard substrates: varied examples from the Oligocene of Antigua, Lesser Antilles
1055 Proceedings of the Geologists' Association, v.128, p.326–331.
- 1056 Erikson, J.P., Pindell, J.L., Larue, D.K., 1990, Mid-Eocene-Early Oligocene Sinistral
1057 Transcurrent Faulting in Puerto Rico Associated with Formation of the Northern
1058 Caribbean Plate Boundary Zone. The Journal of Geology, v.98, p.365–384.
1059 <https://doi.org/10.1086/629410>
- 1060 Favier, A., Lardeaux, J.-M., Legendre, L., Verati, C., Philippon, M., Corsini, M., Münch, P.,
1061 Ventalon, S., 2019, Tectono-metamorphic evolution of shallow crustal levels within
1062 active volcanic arcs. Insights from the exhumed Basal Complex of Basse-Terre
1063 (Guadeloupe, French West Indies). Bulletin de la Société Géologique de France,
1064 v.190, no.10. <https://doi.org/10.1051/bsgf/2019011>
- 1065 Ferrari, L., Petrone, C.M., Francalanci, L., 2001, Generation of oceanic-island basalt-type

- 1066 volcanism in the western Trans-Mexican volcanic belt by slab rollback,
1067 asthenosphere infiltration, and variable flux melting. *Geology* v.29, no.6, p.507-510.
1068 [https://doi.org/10.1130/0091-7613\(2001\)029<0507:GOOIBT>2.0.CO;2](https://doi.org/10.1130/0091-7613(2001)029<0507:GOOIBT>2.0.CO;2)
- 1069 Ferrari, L., Orozco-Esquivel, T., Manea, V., Manea, M., 2012, The dynamic history of the
1070 Trans-Mexican Volcanic Belt and the Mexico subduction zone. *Tectonophysics*, p.
1071 522–523, 122–149. <https://doi.org/10.1016/j.tecto.2011.09.018>
- 1072 Fleck, R. J., Sutter, J. F., & Elliot, D. H., 1977, Interpretation of discordant $^{40}\text{Ar}/^{39}\text{Ar}$ age-
1073 spectra of Mesozoic tholeiites from Antarctica. *Geochimica et Cosmochimica Acta*,
1074 v.41, no.1, p.15-32.
- 1075 Frost, S.H., Weiss, M.P., 1979, Patch reef communities and succession in the Oligocene of
1076 Antigua, West Indies. *Geol. Soc. Amer. Bull.*,v. 90, p.1094-1141.
- 1077 Fox, P. J., Schreiber, E., & Heezen, B. C.,1971. The geology of the Caribbean crust: Tertiary
1078 sediments, granitic and basic rocks from the Aves Ridge. *Tectonophysics*, vol.12,
1079 no.2, p.89-109
- 1080 Gallagher, K., 2012, Transdimensional inverse thermal history modeling for quantitative
1081 thermochronology. *Journal of Geophysical Research : Solid Earth*, v.117(B2).
1082 <https://doi.org/10.1029/2011JB008825>
- 1083 Garrocq, C., Lallemand, S., Marcaillou, B., Lebrun, J. F., Padron, C., Klingelhofer, F., ... &
1084 GARANTI Cruise Team., 2021, Genetic relations between the Aves Ridge and the
1085 Grenada back- arc Basin, East Caribbean Sea. *Journal of Geophysical Research:*
1086 *Solid Earth*, v.126, no.2, e2020JB020466.
- 1087 Germa, A., Quidelleur, X., Labanieh, S., Chauvel, C., Lahitte, P., 2011, The volcanic
1088 evolution of Martinique Island: Insights from K–Ar dating into the Lesser Antilles arc
1089 migration since the Oligocene. *Journal of Volcanology and Geothermal Research*
1090 v.208, p.122–135. <https://doi.org/10.1016/j.jvolgeores.2011.09.007>
- 1091 Gerya, T.V., Fossati, D., Cantieni, C., Seward, D., 2009, Dynamic effects of aseismic ridge
1092 subduction: numerical modelling. *European Journal of Mineralogy*, v.21, p.649–661.
1093 <https://doi.org/10.1127/0935-1221/2009/0021-1931>

- 1094 Glazner, A. F., Walker, J. D., Farmer, G. L., & Bowers, T. D., 2004, The curious
1095 decoupling of magmatism and plate tectonics during the Cenozoic in western North
1096 America: Insight from the Navdat database. In AGU Fall Meeting Abstracts, v.2004,
1097 pp. SF32A-04.
- 1098 Govers, R., Wortel, M.J.R., 2005, Lithosphere tearing at STEP faults: response to edges of
1099 subduction zones. *Earth and Planetary Science Letters*, v.236, p.505–523.
1100 <https://doi.org/10.1016/j.epsl.2005.03.022>
- 1101 Gradstein, F.M., Ogg, J.G., Hilgen, F.J., 2012, On The Geologic Time Scale. No. 45, p.171–
1102 188. <https://doi.org/10.1127/0078-0421/2012/0020>
- 1103 Granja Bruña, J.L., Muñoz-Martín, A., ten Brink, U.S., Carbó-Gorosabel, A., Llanes Estrada,
1104 P., Martín-Dávila, J., Córdoba-Barba, D., Catalán Morollón, M., 2010, Gravity
1105 modeling of the Muertos Trough and tectonic implications (north-eastern Caribbean).
1106 *Marine Geophysical Research*, v.31, p.263–283. [https://doi.org/10.1007/s11001-010-](https://doi.org/10.1007/s11001-010-9107-8)
1107 [9107-8](https://doi.org/10.1007/s11001-010-9107-8)
- 1108 Gunn, B.M., Roobol, M.J., 1976, Metasomatic alteration of the predominantly island arc
1109 igneous suite of the Limestone Caribbees (E. Caribbean). *Geologische Rundschau*,
1110 v.65, p.1078–1108. <https://doi.org/10.1007/BF01808512>
- 1111 Gutscher, M.-A., Spakman, W., Bijwaard, H., Engdahl, E.R., 2000, Geodynamics of flat
1112 subduction: Seismicity and tomographic constraints from the Andean margin.
1113 *Tectonics*, v.19, p.814–833. <https://doi.org/10.1029/1999TC001152>
- 1114 Harford, C. L., Pringle, M. S., Sparks, R. S. J., and Young, S. R., 2002, The volcanic
1115 evolution of Montserrat using $^{40}\text{Ar}/^{39}\text{Ar}$ geochronology: Geological Society,
1116 London, *Memoirs*, v. 21, no.1, p. 93- 113, doi:10.1144/gsl.mem.2002.021.01.05.
- 1117 Hatter, S.J., Palmer, M.R., Gernon, T.M., Taylor, R.N., Cole, P.D., Barfod, D.N., Coussens,
1118 M., 2018, The Evolution of the Silver Hills Volcanic Center, and Revised $^{40}\text{Ar}/^{39}\text{Ar}$
1119 Geochronology of Montserrat, Lesser Antilles, With Implications for Island Arc
1120 Volcanism. *Geochemistry, Geophysics, Geosystems*, v.19, p.427–452.
1121 <https://doi.org/10.1002/2017GC007053>

- 1122 Hutton, C. O., and Nockolds, S. R., 1978, The petrology of Nevis, Leeward Islands, West
1123 Indies: Overseas Geology and Mineral Resources, no. 52, p. 1- 31.
- 1124 Iturralde-Vinent, M., & MacPhee, R. D., 1999, Paleogeography of the Caribbean region:
1125 implications for Cenozoic biogeography. Bulletin of the AMNH: no. 238.
- 1126 Iturralde-Vinent, M., Díaz Otero, C., García-Casco, A. and van Hinsbergen, D.J.J., 2008,
1127 Paleogene Foredeep Basin Deposits of North-Central Cuba: A Record of Arc-
1128 Continent Collision between the Caribbean and North American Plates. International
1129 Geology Review, v.40, p.1-22.
- 1130 Jackson, T.A., 2013, A review of volcanic island evolution and magma production rate: an
1131 example from a Cenozoic island arc in the Caribbean. Journal of the Geological
1132 Society 170, 547–556. <https://doi.org/10.1144/jgs2011-166>
- 1133 Jelínek, V., & Kropáček, V., 1978, Statistical processing of anisotropy of magnetic
1134 susceptibility measured on groups of specimens. Studia geophysica et geodaetica, v.
1135 22, p. 50-62.
- 1136 Jolly, W., Lidiak, E., Schellekens, J., and Santos, H., 1998, Volcanism, tectonics, and
1137 stratigraphic correlations in Puerto Rico, Special Paper 322: Tectonics and
1138 geochemistry of the Northeastern Caribbean, Geological Society of America, p.
1139 1- 34.
- 1140 Kay, S.M., Coira, B.L., 2009, Shallowing and steepening subduction zones, continental
1141 lithospheric loss, magmatism, and crustal flow under the Central Andean Altiplano-
1142 Puna Plateau, in: Backbone of the Americas: Shallow Subduction, Plateau Uplift, and
1143 Ridge and Terrane Collision. Geological Society of America, v.204, p.229
1144 [https://doi.org/10.1130/2009.1204\(11\)](https://doi.org/10.1130/2009.1204(11))
- 1145 Koppers, A.A.P., 2002, ArArCALCF software for $^{40}\text{Ar}/^{39}\text{Ar}$ age calculations, Computers
1146 and Geosciences, v.28, no.5, p.605-619.
- 1147 Laó-Dávila, D.A., 2014, Collisional zones in Puerto Rico and the northern Caribbean. Journal
1148 of South American Earth Sciences, v.54, p.1–19.
1149 <https://doi.org/10.1016/j.jsames.2014.04.009>

- 1150 Laurencin, M., Marcaillou, B., Graindorge, D., Klingelhoefer, F., Lallemand, S., Laigle, M.,
1151 Lebrun, J.-F., 2017, The polyphased tectonic evolution of the Anegada Passage in the
1152 northern Lesser Antilles subduction zone. *Tectonics*, v.36, p.945–961.
1153 <https://doi.org/10.1002/2017TC004511>
- 1154 Lee, S. H., Iza, F., & Lee, J. K., 2006, Particle-in-cell Monte Carlo and fluid simulations of
1155 argon-oxygen plasma: Comparisons with experiments and validations. *Physics of*
1156 *plasmas*, v.13, no.5, p.57-102.
- 1157 Legendre, L., Philippon, M., Münch, Ph., Leticée, J.L., Noury, M., Maincent, G., Cornée, J.J.,
1158 Caravati, A., Lebrun, J.F., Mazabraud, Y., 2018, Trench Bending Initiation: Upper
1159 Plate Strain Pattern and Volcanism. Insights From the Lesser Antilles Arc, St.
1160 Barthelemy Island, French West Indies. *Tectonics*, v.37, p.2777–2797.
1161 <https://doi.org/10.1029/2017TC004921>
- 1162 Le Guen de Kerneizon, M., Bellon, H., Carron, J.-P., Maury, R., 1983, L'île de Sainte Lucie
1163 (Petites Antilles): distinction des principales séries magmatiques à partir des données
1164 pétrochimiques et géochronologiques. *Bulletin de la Société Géologique de France* 7
1165 (XXV, no 6), p.845–853.
- 1166 Leroy, S., Mauffret, A., Patriat, P., Mercier de Lepinay, B., 2000, An alternative
1167 interpretation of the Cayman trough evolution from a reidentification of magnetic
1168 anomalies. *Geophysical Journal International*, v.141, p.539–557.
1169 <https://doi.org/10.1046/j.1365-246x.2000.00059.x>
- 1170 Li, Z.X., Bogdanova, S.V., Collins, A.S., Davidson, A., De Waele, B., Ernst, R.E.,
1171 Fitzsimons, I.C.W., Fuck, R.A., Gladkochub, D.P., Jacobs, J., Karlstrom, K.E., Lu,
1172 S., Natapov, L.M., Pease, V., Pisarevsky, S.A., Thrane, K., Vernikovsky, V., 2008,
1173 Assembly, configuration, and break-up history of Rodinia: A synthesis. *Precambrian*
1174 *Research*, v.160, p.179–210. <https://doi.org/10.1016/j.precamres.2007.04.021>
- 1175 Lindsay, J.M., Trumbull, R.B., Schmitt, A.K., Stockli, D.F., Shane, P.A., Howe, T.M., 2013.

- 1176 Volcanic stratigraphy and geochemistry of the Soufrière Volcanic Centre, Saint Lucia
1177 with implications for volcanic hazards. *Journal of Volcanology and Geothermal*
1178 *Research* 258, 126–142. <https://doi.org/10.1016/j.jvolgeores.2013.04.011>
- 1179 Ma, X., Attia, S., Cawood, T., Cao, W., Xu, Z., & Li, H., 2022, Arc Tempos of the Gangdese
1180 Batholith, Southern Tibet. *Journal of Geodynamics*, 101897 (in press).
- 1181 Macdonald, R., Hawkesworth, C.J., Heath, E., 2000, The Lesser Antilles volcanic chain: a
1182 study in arc magmatism. *Earth-Science Reviews*, v.49, p.1–76.
1183 [https://doi.org/10.1016/S0012-8252\(99\)00069-0](https://doi.org/10.1016/S0012-8252(99)00069-0)
- 1184 Maffione, M., Hernandez-Moreno, C., Ghiglione, M.C., Speranza, F., van Hinsbergen, D.J.J.,
1185 Lodolo, E., 2015, Constraints on deformation of the Southern Andes since the
1186 Cretaceous from anisotropy of magnetic susceptibility. *Tectonophysics*, v.665,
1187 p.236–250. <https://doi.org/10.1016/j.tecto.2015.10.008>
- 1188 Mann, P., Calais, E., Ruegg, J.-C., DeMets, C., Jansma, P.E., Mattioli, G.S., 2002, Oblique
1189 collision in the northeastern Caribbean from GPS measurements and geological
1190 observations,. *Tectonics*, v.21, p.1–26. <https://doi.org/10.1029/2001TC001304>
- 1191 Marivaux, L., Vélez-Juarbe, J., Merzeraud, G., Pujos, F., Vinola Lopez, L. W., Boivin, M.,
1192 Santos-Mercado, H., Cruz, E.J., Grajales A., Padilla J., Vélez-Rosado, K.I.,
1193 Philippon, M., Léticée, J.L., Münch, P., Antoine, P.O., 2020, Early Oligocene
1194 chinchilloid caviomorphs from Puerto Rico and the initial rodent colonization of the
1195 West Indies. *Proceedings of the Royal Society Bulletin*, v.287, no.1920,.
- 1196 Martinod, J., Guillaume, B., Espurt, N., Faccenna, C., Funicello, F., Regard, V., 2013, Effect
1197 of aseismic ridge subduction on slab geometry and overriding plate deformation:
1198 Insights from analogue modeling. *Tectonophysics*, v. 588, p.39–55.
1199 <https://doi.org/10.1016/j.tecto.2012.12.010>
- 1200 Martin-Kaye, P.H.A., 1959, Reports on the geology of the Leeward and British Virgin
1201 Islands. Voice Publishing Co., Ltd., St. Lucia, W.I., p.117.
- 1202 Martin-Kaye, P.H.A., 1969, A summary of the geology of the Lesser Antilles. *Overseas*
1203 *Geology and Mineral Resources* , v.10, p.172-206.

- 1204 Mascle, A., Westercamp, D., 1983, Geologie d'Antigua, Petites Antilles. Bulletin de la
1205 Société Géologique de France S7-XXV, p.855–866.
1206 <https://doi.org/10.2113/gssgfbull.S7-XXV.6.855>
- 1207 Multer, H.G., Weiss, M.P., Nicholson, D.V., 1986, Antigua; reefs, rocks and highroads of
1208 history. Leeward Island Science Associates, St John's, Antigua, Contrib., v.1, p.116
- 1209 McCann, W.R., Sykes, L.R., 1984, Subduction of aseismic ridges beneath the Caribbean
1210 Plate: Implications for the tectonics and seismic potential of the northeastern
1211 Caribbean. Journal of Geophysical Research, v..89, p.4493–4519.
1212 <https://doi.org/10.1029/JB089iB06p04493>
- 1213 McCarthy, A., Tugend, J., Mohn, G., Candiotti, L., Chelle-Michou, C., Arculus, R.,
1214 Schmalholz, S.M., Müntener, O., 2020, A case of Ampferer-type subduction and
1215 consequences for the Alps and the Pyrenees. American Journal of Sciences, v.320,
1216 p.313–372. <https://doi.org/10.2475/04.2020.01>
- 1217 McGeary, S., Nur, A., Ben-Avraham, Z., 1985, Spatial gaps in arc volcanism: The effect of
1218 collision or subduction of oceanic plateaus. Tectonophysics, v.119, p.195–221.
1219 [https://doi.org/10.1016/0040-1951\(85\)90039-3](https://doi.org/10.1016/0040-1951(85)90039-3)
- 1220 Meighan, H. E., Pulliam, J., ten Brink, U., & López- Venegas, A. M., 2013, Seismic
1221 evidence
1222 for a slab tear at the Puerto Rico Trench. Journal of Geophysical Research: Solid
1223 Earth, v.118, no.6, p.2915-2923.
- 1224 Meredith, A.S., Williams, S.E., Collins, A.S., Tetley, M.G., Mulder, J.A., Blades, M.L.,
1225 Young, A., Armistead, S.E., Cannon, J., Zahirovic, S., Müller, R.D., 2021, Extending
1226 full-plate tectonic models into deep time: Linking the Neoproterozoic and the
1227 Phanerozoic. Earth-Science Reviews, v.214, no.103477.
1228 <https://doi.org/10.1016/j.earscirev.2020.103477>
- 1229 Miller, K. G., Browning, J. V., Schmelz, W. J., Kopp, R. E., Mountain, G. S., & Wright, J. D.,

- 1230 2020, Cenozoic sea-level and cryospheric evolution from deep-sea geochemical and
1231 continental margin records. *Science advances*, v.6, no.20.
- 1232 Mohn, G., Karner, G.D., Manatschal, G., Johnson, C.A., 2015, Structural and stratigraphic
1233 evolution of the Iberia–Newfoundland hyper-extended rifted margin: a quantitative
1234 modelling approach. *Geological Society of London, Special Publications*, v.413,
1235 p.53–89. <https://doi.org/10.1144/SP413.9>
- 1236 Montes, C., Rodriguez-Corcho, A.F., Bayona, G., Hoyos, N., Zapata, S. and Cardona, A.,
1237 2019. Continental margin response to multiple arc-continent collisions: The northern
1238 Andes-Caribbean margin. *Earth-Science Reviews*, no.102903.
- 1239 Moore, J.G., 1970, Relationship between subsidence and volcanic load, Hawaii: *Bulletin*
1240 *Volcanologique*, v. 34, no. 2, p. 562–576, <https://doi.org/10.1007/BF02596771>
- 1241 Multer, H.G., Weiss, M.P., Nicholson, D.V., 1986, Antigua; reefs, rocks and highroads of
1242 history. *Leeward Island Science Associates, St John's, Antigua, Contrib.* v.1, p.116
- 1243 Münch, P., Lebrun, J.-Frédéric., Cornée, J.-J., Thinon, I., Guennoc, P., Marcaillou, B.J.,
1244 Begot, J., Bertrand, G., De Berc, S.B., Biscarrat, K., Claud, C., De Min, L., Fournier,
1245 F., Gailler, L., Graindorge, D., Léticée, J.-L., Marie, L., Mazabraud, Y., Melinte-
1246 Dobrinescu, M., Moissette, P., Quillévéré, F., Verati, C., Randrianasolo, A., 2013,
1247 Pliocene to Pleistocene carbonate systems of the Guadeloupe archipelago, French
1248 Lesser Antilles: a land and sea study (the KaShallow project). *Bulletin de la Société*
1249 *Géologique de France*, v.184, p.99–110. <https://doi.org/10.2113/gssgfbull.184.1-2.99>
- 1250 Nagle, F., Stipp, J.J., Fisher, D.E., 1976, K-Ar geochronology of the Limestone Caribbees
1251 and Martinique, Lesser Antilles, West Indies. *Earth and Planetary Science Letters*,
1252 v.29, p.401–412. [https://doi.org/10.1016/0012-821X\(76\)90145-X](https://doi.org/10.1016/0012-821X(76)90145-X)
- 1253 Nemec, W., Steel, R. J., 1984, Alluvial and coastal conglomerates: their significant features
1254 and some comments on gravelly mass-flow deposits. In: Koster, E.H., Steel, R.J.
1255 (Eds.), *Sedimentology of Gravels and Conglomerates*. *Mem. Can. Soc. Petrol. Geol.*,
1256 v.10.
- 1257 Noury, M., Philippon, M., Cornée, J., Bernet, M., Bruguier, O., Montheil, L., Legendre, L.,

- 1258 Dugamin, E., Bonno, M., Münch, P., 2021, Evolution of a Shallow Volcanic Arc
1259 Pluton During Arc Migration: A Tectono - Thermal Integrated Study of the St.
1260 Martin Granodiorites (Northern Lesser Antilles). *Geochemistry, Geophysics,*
1261 *Geosystems*, v.22. <https://doi.org/10.1029/2020GC009627>
- 1262 Padron, C., Klingelhoefer, F., Marcaillou, B., Lebrun, J. F., Lallemand, S., Garrocq, C., Laigle,
1263 M., Roest, W.R., Beslier, M.O., Schenini, L., Graindorge, D., Gay, A., Audemard, F.,
1264 Münch, P., 2021, Deep structure of the Grenada Basin from wide-angle seismic,
1265 bathymetric and gravity data. *Journal Of Geophysical Research : Solid Earth*,
1266 v.126, no.2.
- 1267 Parés, J.M., van der Pluijm, B.A., Dinarès-Turell, J., 1999, Evolution of magnetic fabrics
1268 during incipient deformation of mudrocks (Pyrenees, northern Spain).
1269 *Tectonophysics*, v.307, p.1–14. [https://doi.org/10.1016/S0040-1951\(99\)00115-8](https://doi.org/10.1016/S0040-1951(99)00115-8)
- 1270 Parsons, A.J., Sigloch, K., Hosseini, K., 2021, Australian Plate Subduction is Responsible for
1271 Northward Motion of the India - Asia Collision Zone and ~1,000 km Lateral
1272 Migration of the Indian Slab. *Geophysical Research Letters*, v.48.
1273 <https://doi.org/10.1029/2021GL094904>
- 1274 Pearce, J. A., Peate, D. W., 1995, Tectonic implications of the composition of volcanic arc
1275 magmas. *Annual review of Earth and planetary sciences*, v.23, no.1, p.251-285
- 1276 Persad, K.M., 1969, Stratigraphy, paleontology and paleoecology of the Antigua Formation.
1277 Unpublished, University of the West Indies Ph.D. dissertation, 222 p., Kingston,
1278 Jamaica.
- 1279 Philippon, M., Cornée, J.-J., Münch, P., van Hinsbergen, D.J.J., BouDagher-Fadel, M.,
1280 Gailler, L., Boschman, L.M., Quillevère, F., Montheil, L., Gay, A., Lebrun, J.F.,
1281 Lallemand, S., Marivaux, L., Antoine, P.-O., with the GARANTI Team, 2020a,
1282 Eocene intra-plate shortening responsible for the rise of a faunal pathway in the
1283 northeastern Caribbean realm. *PLoS ONE*, v.15, no.0241000.
1284 <https://doi.org/10.1371/journal.pone.0241000>

- 1285 Philippon, M., van Hinsbergen, D.J.J., Boschman, L.M., Gossink, L.A.W., Cornée, J.-J.,
1286 BouDagher-Fadel, M., Léticée, J.-L., Lebrun, J.-F., Munch, P., 2020b, Caribbean
1287 intra-plate deformation: Paleomagnetic evidence from St. Barthélemy Island for post-
1288 Oligocene rotation in the Lesser Antilles forearc. *Tectonophysics*, v.777, no.228323.
1289 <https://doi.org/10.1016/j.tecto.2020.228323>
- 1290 Pindell, J., Dewey, J.F., 1982, Permo-Triassic reconstruction of western Pangea and the
1291 evolution of the Gulf of Mexico/Caribbean region. *Tectonics*, v.1, p.179–211.
1292 <https://doi.org/10.1029/TC001i002p00179>
- 1293 Pindell, J.L., Kennan, L., 2009, Tectonic evolution of the Gulf of Mexico, Caribbean and
1294 northern South America in the mantle reference frame: an update. Geological
1295 Society, London, Special Publications, v.328, p.1–55.
1296 <https://doi.org/10.1144/SP328.1>
- 1297 Rankin, D. W., 2002, Geology of St. John, US Virgin Islands, US Geological Survey, U.S.
1298 Geological 531 Survey Professional Paper.
- 1299 Renne, P.R., Balco, G., Ludwig, K.R., Mundil, R., Min, K., 2011, Response to the comment
1300 by W.H. Schwarz et al. on “Joint determination of 40K decay constants and
1301 40Ar*/40K for the Fish Canyon sanidine standard, and improved accuracy for
1302 40Ar/39Ar geochronology” by P.R. Renne et al. (2010). *Geochimica et*
1303 *Cosmochimica Acta*, v.75, p.5097–5100. <https://doi.org/10.1016/j.gca.2011.06.021>
- 1304 Robinson, E., Paytan, A., Chein, C.-T., 2017, Strontium isotope dates for the Oligocene
1305 Antigua Formation, Antigua, W. I. Caribbean Journal of Earth Science 50, 11-18.
- 1306 Rojas-Agramonte, Y., Williams, I.S., Arculus, R., Kröner, A., García-Casco, A., Lázaro, C.,
1307 Buhre, S., Wong, J., Geng, H., Echeverría, C.M., Jeffries, T., Xie, H., Mertz-Kraus,
1308 R., 2017, Ancient xenocrystic zircon in young volcanic rocks of the southern Lesser
1309 Antilles island arc. *Lithos*, v.290–291, p.228–252.
1310 <https://doi.org/10.1016/j.lithos.2017.08.002>
- 1311 Rosenbaum, G., Caulfield, J.T., Ubide, T., Ward, J.F., Sandiford, D., Sandiford, M., 2021,

- 1312 Spatially and Geochemically Anomalous Arc Magmatism: Insights From the Andean
1313 Arc. *Geochemistry, Geophysics, Geosystems*, v.22.
1314 <https://doi.org/10.1029/2021GC009688>
- 1315 Samper, A., Quidelleur, X., Lahitte, P., Mollex, D., 2007, Timing of effusive volcanism and
1316 collapse events within an oceanic arc island: Basse-Terre, Guadeloupe archipelago
1317 (Lesser Antilles Arc). *Earth and Planetary Science Letters*, v.258, p.175–191.
1318 <https://doi.org/10.1016/j.epsl.2007.03.030>
- 1319 Schepers, G., van Hinsbergen, D.J.J., Spakman, W., Kosters, M.E., Boschman, L.M. and
1320 McQuarrie, N., 2017,. South-American plate advance and forced Andean trench
1321 retreat as drivers for transient flat subduction episodes. *Nature communications*, v.8,
1322 no.15249.
- 1323 Schlaphorst, D., Melekhova, E., Kendall, J. M., Blundy, J., & Latchman, J. L., 2018, Probing
1324 layered arc crust in the Lesser Antilles using receiver functions. *Royal Society open
1325 science*, v.5, no.11.
- 1326 Schrecengost, K. L., 2010,. *Geochemistry and uranium/lead zircon geochronology of the
1327 Virgin Islands batholith, British Virgin Islands (PhD thesis)*, The University of North
1328 Carolina at Chapel Hill.
- 1329 Smith, A. L., Roobol, M. J., Mattioli, G. S., Fryxell, J. E., Daly, G. E., & Fernandez, L. A.
1330 2013, *The volcanic geology of the mid-arc Island of Dominica*, Geological Society of
1331 America, v.496.
- 1332 Spakman, W., Chertova, M.V., van den Berg, Arie., van Hinsbergen, D.J.J., 2018, Puzzling
1333 features of western Mediterranean tectonics explainedby slab dragging. *Nature
1334 Geoscience*, v.11, p.211–216. <https://doi.org/10.1038/s41561-018-0066-z>
- 1335 Speed, R. C., Smith-Horowitz, P. L., Perch-Nielsen, K. V. S., & Sanfilippo, A. B., 1993,
1336 *Southern Lesser Antilles Arc Platform: pre-late Miocene stratigraphy, structure, and
1337 tectonic evolution* , Geological Society of America, v.277.
- 1338 Stern, R.J., Reagan, M., Ishizuka, O., Ohara, Y. and Whattam, S., 2012, To understand

- 1339 subduction initiation, study forearc crust: To understand forearc crust, study
1340 ophiolites. *Lithosphere*, v.4, no.6, p.469-483.
- 1341 Strang, K.M., Harper, D.A.T., Donovan, S.K., 2018, Silicification of low-magnesium mollusc
1342 shells from the Upper Oligocene of Antigua, Lesser Antilles. *Caribbean Journal of*
1343 *Earth Science*, v.50, p.37-43.
- 1344 Symithe, S., Calais, E., de Chabaliere, J.B., Robertson, R., Higgins, M., 2015. Current block
1345 motions and strain accumulation on active faults in the Caribbean: CURRENT
1346 CARIBBEAN KINEMATICS. *Journal of Geophysical Research. Solid Earth* 120,
1347 3748–3774. <https://doi.org/10.1002/2014JB011779>
- 1348 Tallarico, A., Dragoni, M., Anzidei, M., and Esposito, A., 2003, Modeling long-term ground
1349 deformation due to the cooling of a magma chamber: Case of Basiluzzo island,
1350 Aeolian Islands, Italy: *Journal of Geophysical Research. Solid Earth*, v. 108, no. B12,
1351 <https://doi.org/10.1029/2002JB002376>.
- 1352 Tatsumi, Y., Sakuyama, M., Fukuyama, H., Kushiro, I., 1983, Generation of arc basalt
1353 magmas and thermal structure of the mantle wedge in subduction zones. *Journal of*
1354 *Geophysical Research*, v.88, p.5815–5825. <https://doi.org/10.1029/JB088iB07p05815>
- 1355 Thomas, H.D., 1942, On fossils from Antigua, and the age of the Seaforth Limestone.
1356 *Geological Magazine*, v.79, p.49-61. doi.org/10.1017/S0016756800073490
- 1357 Trechmann, C.T., 1933, The Uplift of Barbados. *Geological Magazine*, v.70, p.19–47.
1358 <https://doi.org/10.1017/S0016756800091214>
- 1359 Trechmann, C.T., 1941, Some observations on the geology of Antigua, West Indies.
1360 *Geological Magazine* v.78, p.113-124.
- 1361 van Benthem, S., Govers, R., Spakman, W., Wortel, R., 2013. Tectonic evolution and mantle
1362 structure of the Caribbean, *Journal of Geophysical Research : Solid Earth*, v.118,
1363 p.3019–3036. <https://doi.org/10.1002/jgrb.50235>
- 1364 van Benthem, S., Govers, R. and Wortel, R., 2014, What drives microplate motion and
1365 deformation in the northeastern Caribbean plate boundary region? *Tectonics*, v.33,
1366 no.5, p.850-873.

- 1367 van den Bold, W.A., 1966, Ostracoda from the Antigua Formation (Oligocene, Lesser
1368 Antilles). *Journal of Paleontology*, v.40, p.1233-1236.
- 1369 van de Lagemaat, S.H.A., van Hinsbergen, D.J.J., Boschman, L.M., Kamp, P.J.J., Spakman,
1370 W., 2018, Southwest Pacific Absolute Plate Kinematic Reconstruction Reveals Major
1371 Cenozoic Tonga-Kermadec Slab Dragging. *Tectonics*, v.37, p.2647–2674.
1372 <https://doi.org/10.1029/2017TC004901>
- 1373 van Hunen, J., van den Berg, A.P., Vlaar, N.J., 2002, On the role of subducting oceanic
1374 plateaus in the development of shallow flat subduction. *Tectonophysics*, v.352,
1375 p.317–333. [https://doi.org/10.1016/S0040-1951\(02\)00263-9](https://doi.org/10.1016/S0040-1951(02)00263-9)
- 1376 Vaughan, T.W., 1919, Fossil corals from Central America, Cuba, and Puerto Rico with an
1377 account of the American Tertiary, Pleistocene, and Recent coral reefs. *U.S. National*
1378 *Museum Bulletin*, v.103, p.189-524.
- 1379 Weiss, M.P., 1994, Oligocene limestones of Antigua, West Indies: Neptune succeeds Vulcan.
1380 *Caribbean Journal of Earth Sciences*, v.30, p.1-29.
- 1381 White, W., Copeland, P., Gravatt, D.R., Devine, J.D., 2017, Geochemistry and geochronology
1382 of Grenada and Union islands, Lesser Antilles: The case for mixing between two
1383 magma series generated from distinct sources. *Geosphere*, v.13, p.1359–1391.
1384 <https://doi.org/10.1130/GES01414.1>
- 1385 Yang, T.F., Lee, T., Chen, C.-H., Cheng, S.-N., Knittel, U., Punongbayan, R.S., Rasdas, A.R.,
1386 1996, A double island arc between Taiwan and Luzon: consequence of ridge
1387 subduction. *Tectonophysics*, v.258, p.85–101. [https://doi.org/10.1016/0040-](https://doi.org/10.1016/0040-1951(95)00180-8)
1388 [1951\(95\)00180-8](https://doi.org/10.1016/0040-1951(95)00180-8)
- 1389 Zami, F., Quidelleur, X., Ricci, J., Lebrun, J.-F., Samper, A., 2014, Initial sub-aerial volcanic
1390 activity along the central Lesser Antilles inner arc: New K–Ar ages from Les Saintes
1391 volcanoes. *Journal of Volcanology and Geothermal Research*, v.287, p.12–21.
1392 <https://doi.org/10.1016/j.jvolgeores.2014.09.011>
- 1393 Zhang, X., Chung, S.-L., Lai, Y.-M., Ghani, A.A., Murtadha, S., Lee, H.-Y., Hsu, C.-C.,

1394 2019, A 6000-km-long Neo-Tethyan arc system with coherent magmatic flare-ups
1395 and lulls in South Asia. *Geology*, v.47, p.573–576. <https://doi.org/10.1130/G46172.1>

1396

1397 **APPENDIX**

1398 Appendix 1 : DESCRIPTION OF THE SECTIONS, AGES AND DEPOSITIONAL
1399 SETTINGS;

1400 Appendix 2 : MICROFACIES AND LARGER BENTHIC FORAMINIFERA
1401 CONTENT;

1402 Appendix 3 : DESCRIPTION OF THE SEISMIC PROFILES 508 AND 510

1403 Appendix 4 : STRUCTURAL MEASUREMENTS.

1404 Table of the structural measurements collected in the field. Strikes are expressed
1405 from 0 to 360° following the right hand rule.

1406 Appendix 5 : $^{40}\text{Ar}/^{39}\text{Ar}$ methodology

1407

1408 ¹GSA Data Repository item 201Xxxx, [Appendix 1 : DESCRIPTION OF
1409 THE SECTIONS, AGES AND DEPOSITIONAL SETTINGS; Appendix 2 :
1410 MICROFACIES AND LARGER BENTHIC FORAMINIFERA CONTENT;
1411 Appendix 3 : DESCRIPTION OF THE SEISMIC PROFILES 508 AND
1412 510], is available online at www.geosociety.org/pubs/ft20XX.htm, or on
1413 request from editing@geosociety.org.

1414

1415